LA-UR- 11-00984

Approved for public release; distribution is unlimited.

Title:	In-situ electromagnetic gauging and its application to shock compression science and detonation physics
Author(s):	Dana M. Dattelbaum Stephen A. Sheffield Richard L. Gustavsen
Intended for:	Institute of Shock Physics - Diagnostics workshop Imperial College, London, U.K. Feb. 17, 2011

Los Alamos
NATIONAL LABORATORY
EST. 1943

Los Alamos National Laboratory, an affirmative action/equal opportunity employer, is operated by the Los Alamos National Security, LLC for the National Nuclear Security Administration of the U.S. Department of Energy under contract DE-AC52-06NA25396. By acceptance of this article, the publisher recognizes that the U.S. Government retains a nonexclusive, royalty-free license to publish or reproduce the published form of this contribution, or to allow others to do so, for U.S. Government purposes. Los Alamos National Laboratory requests that the publisher identify this article as work performed under the auspices of the U.S. Department of Energy. Los Alamos National Laboratory strongly supports academic freedom and a researcher's right to publish; as an institution, however, the Laboratory does not endorse the viewpoint of a publication or guarantee its technical correctness.

Form 836 (7/06)

Abstract

Electromagnetic gauging has been applied to problems in shock compression science since the 1940s. Its development dates back to Russia, where it was applied to detonation physics in the 1940s-1960s. Electromagnetic gauges operate on the principle described by Faraday's law, in which a conductor moving in a magnetic field produces a current proportional to its velocity, the conductor length and the magnetic field strength. In this presentation, the details of the application of electromagnetic gauging in shock and detonation physics experiments will be described. Included in the discussion will be details of the sample preparation, data analysis and sources of error. Finally, recent applications in the shock initiation of explosives and shock-induced chemistry of simple organic molecules will be present to demonstrate the utility of the gauges in provided detailed insights into evolving reactive flow.

In-situ electromagnetic gauging and its application in shock compression science and detonation physics

Dana Dattelbaum, Stephen Sheffield, Rick Gustavsen

*Shock and Detonation Physics (WX-9)
Los Alamos National Laboratory
Los Alamos, NM 87545

Institute of Shock Physics – Diagnostics Workshop
Imperial College, London, U.K.
February 17, 2011

Los Alamos NATIONAL LABORATORY EST. 1943 danadat@lanl.gov

What is in-situ electromagnetic gauging?

The use of thin metal foil elements in dynamic experiments to measure:

- *time of arrival (shock, detonation, rarefaction velocities)*
- *shock wave evolution at multiple (Lagrangian) positions*

Time of arrival, waves at interfaces

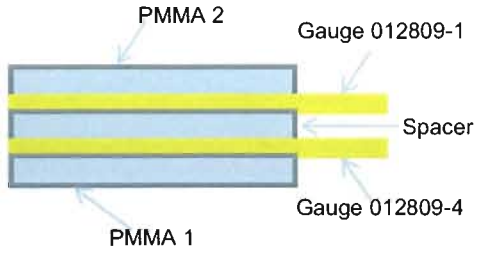

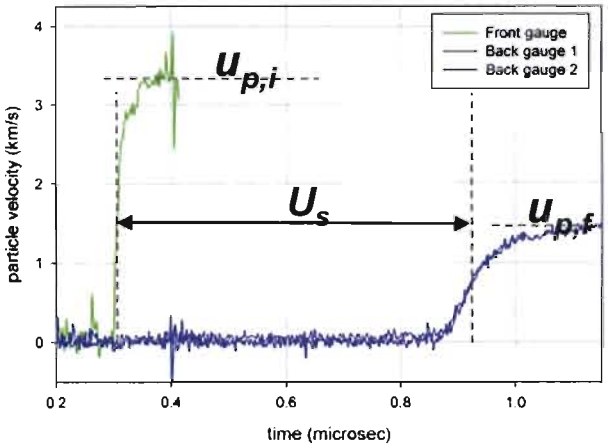

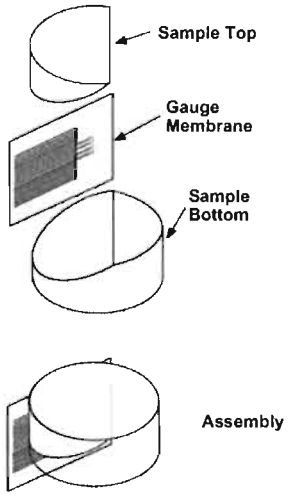

Details of wave evolution In-situ

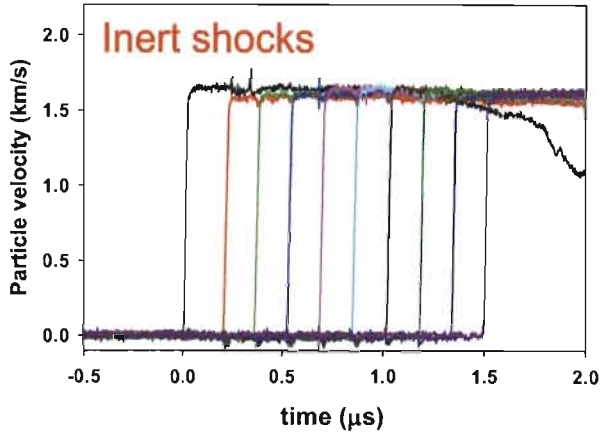

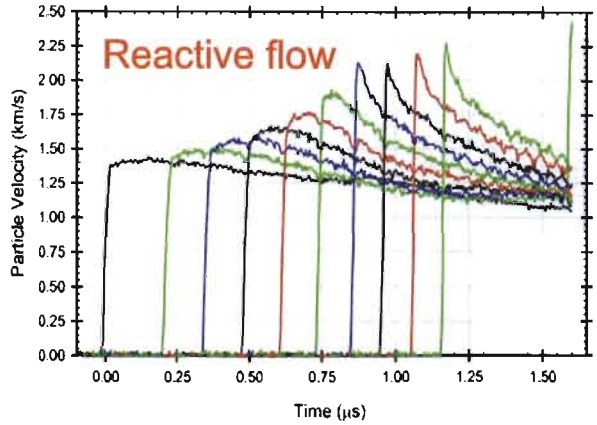

Outline

- History of gauging
  - Russian development, U. S. and LANL History
- Principles of operation
- Advantages/disadvantages
- The “details” of electromagnetic gauging in shock compression experiments
- Data interpretation
- Research examples
  - Hot spots in initiating explosives
  - Shock-induced chemistry

History of Magnetic Gauging

- Invented in Russian (late 1940s)
  - Zaitzev, Pokhil et al. (1960)
  - Reports of use in HEs in early 1960s – Dremin
  - Continued use by Koldunov (Chernogolovka)

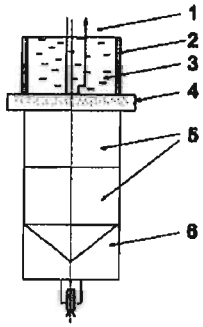

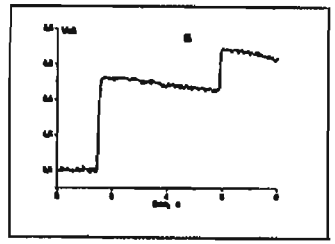

Koldunov et al. – inert shock in NM/NB mixture

- U.S. Work
  - Jacobs & Edwards (1970)
  - Cowperthwaite & Rosenberg (1976)
  - Fowles at PI and WSU in 1970s on guns
  - Vorthman & Wackerle (1980s – LANL)
  - Erickson et al. (early 1980s – LLNL)
  - Gupta et al. SRI – 2D fields and shear measurements (1980)
  - Explosives at LANL (guns) – 1980s-present (Sheffield/Gustavsen)
- CEA – B. Leal-Crouzet, A. Sollier
- U.K. – Cranfield Univ. Cu/Mylar gauges
- Harvard Univ.
- U.S. DoD Labs
  - Army Research Laboratory – Dandekar/Cassem
  - NSWC-Indian Head - Sutherland

Zaitzev, V. M., Pokhil. P. F., and Shvedov, K. K., DAN SSSR, **132**, p. 1339 (1960). Dremin, A. N., and Pokhil, P. F., Zh. Fix. Chimia. 34, 9. 11 (1960). Dremin, A. N., Zaitzev, V. M., Ilyukhin, V. S., and Pokhil, P. F., "Detonation Parameters," Proceedings of the Eighth Symposium on Combustion, Baltimore, MD, p. 610 (1962). Gustavsen, Sheffield, Alcon, Hill, Los Alamos Report # LA-13634-MS. C. Stennett, G. A. Cooper, P. J. Hazell, G. Appleby-Thomas, AIP Conf. Proc., 1195, 267. A. Sollier et al. 14th Int. Det. Symp. pg. 563 (2010). S. A. Koldunov et al. Comb. Expl. Shock Waves, 46, pg. 64 (2010).

Shock waves are pressure discontinuities that propagate in materials.

A shock wave is treated as a "jump" discontinuity - its characteristics are determined by material thermodynamics

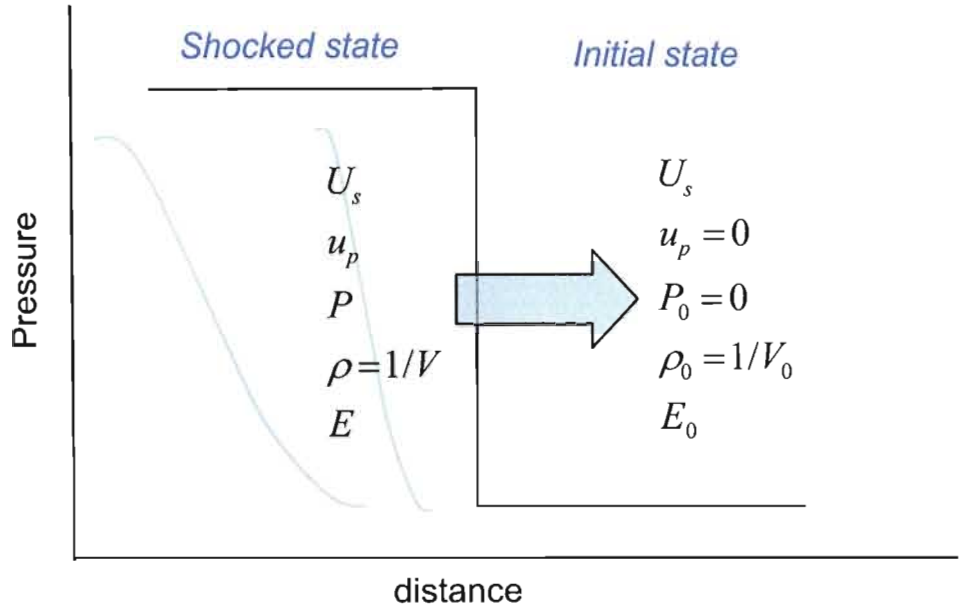

"Jump condition" is constrained by conservation of:

$$\frac{V}{V_0} = \frac{\rho_0}{\rho} = \frac{(U_s - u_p)}{(U_s - u_{p,0})}$$ mass

$$P - P_0 = \rho_0 (U_s - u_{p,0})(u_p - u_{p,0})$$ momentum

$$E - E_0 = \frac{1}{2}(P + P_0)(V_0 - V)$$ energy

Measure 1 variable – need EOS standard
Measure 2 variables – define Hugoniot locus
Mechanical variables only

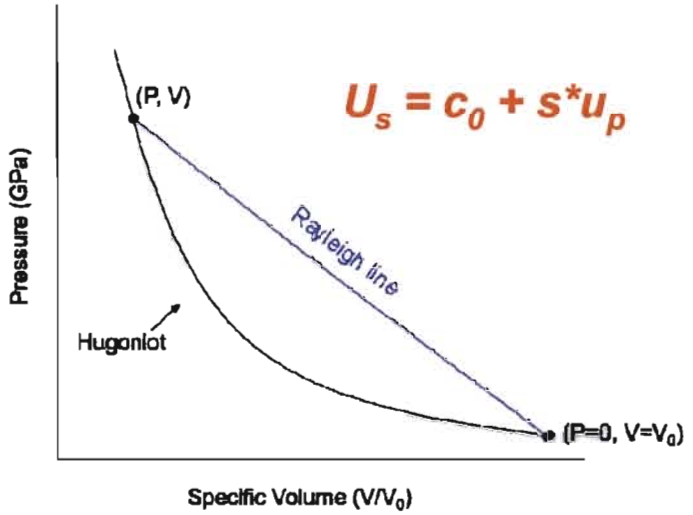

Shock dynamics – methods of measuring Hugoniot locus

- Need to measure U_s, u_p, or P
  - U_s – impedance match off standard
  - u_p – reverse ballistic, impedance match off standard
  - U_s, u_p – measured redundantly with magnetic gauges
- Context of other methods
  - Pins - average velocity, perturbing
  - Embedded fibers – average velocity, perturbing
  - Streak Cameras
  - Laser Velocimetry (VISAR, PDV) – transit time, *interface*
  - Quartz Gauges – Perturbing, limited to interfaces & low pressures
  - In-Situ Gauges
    - Pressure - Manganin (thick), must be calibrated
    - Electromagnetic Gauges –

      thin, no calibration, u_p vs. t (U_s), multiple measurements, matched to PBXs

Not perfect, but close to ideal for certain types of experiments

Advantages/disadvantage of magnetic gauging

- Advantages
  - ✓ Wave profiles are recorded at multiple positions – evolution (unique & powerful)
  - ✓ No calibration of the gauges needed
  - ✓ Minimally perturbative to flow
  - ✓ Robust to harsh conditions (detonation, "hot" samples – foams, porous mat'ls)
  - ✓ Can be used in a variety of configurations (layers, various angles, short shock/long-run)

- Disadvantages
  - × Not for conductive samples or impactors (metals)
  - × Very sensitive to care in assembly/tolerances
  - × Involved and expensive to set-up (experience, cost, gauge manufacturing)
  - × Lower temporal resolution
  - × Requires experienced interpretation
  - × "Noisy" samples – quartz, silica, heterogeneous materials or structures

Electromagnetic gauging is based on principles of Faraday's Law.

$$emf(V) = -\frac{d\phi_m}{dt}$$ *From Maxwell's Eq's*

$$emf(V) = \int_a^b (-\vec{u}_p \times \vec{B}) d\vec{L} = BLu_p \sin(\theta)$$

u_p is conductor velocity
L is conductor length
B is magnetic field strength

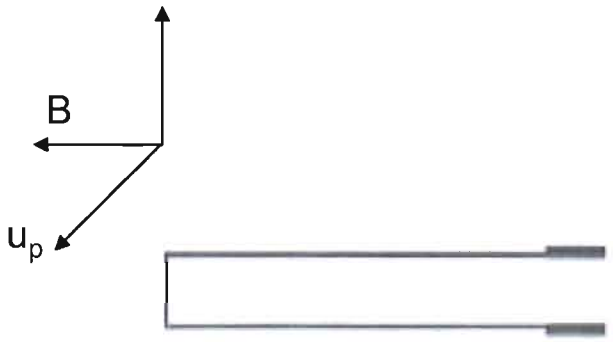

If all vectors are (by design) orthogonal:

$$V = LuB$$

V is induced voltage – ~ 2V in detonating explosive on longest gauge

A (nearly) uniform magnetic field is obtained using Helmholtz coils mounted at the end of our gas gun barrels.

$$B = \frac{32\pi(N)(I)}{5\sqrt{5}a} \times 10^{-7} \quad \text{(tesla)}$$

N = # turns in coil
I = current
a = coil radius
B = magnetic field strength

Increase in coil radius = increase in field strength

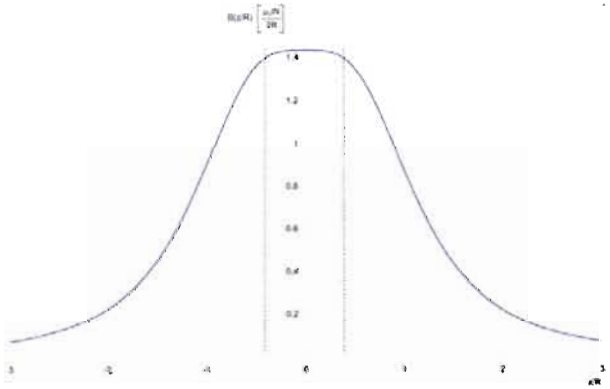

$$B_z(r) = NI \times 10^{-7} \int_0^{2\pi} \frac{2a(a - r\cos(\theta))d\theta}{(a^2 - b^2 + r^2 - 2ar * \cos(\theta))^{3/2}}$$

Coil spacing = field uniformity

(1 tesla = 10,000 G) Helmholtz coil pictures - Wikipedia

Helmholtz coils
(Hermann von Helmholtz, 1821-1894)

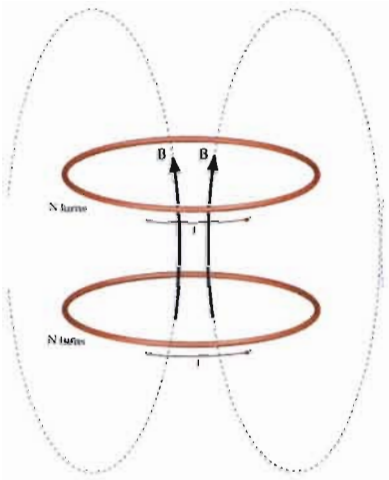

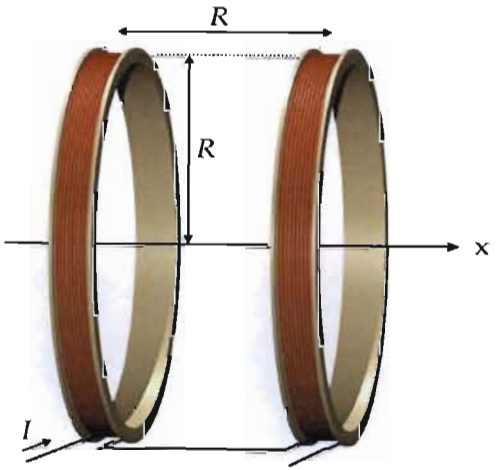

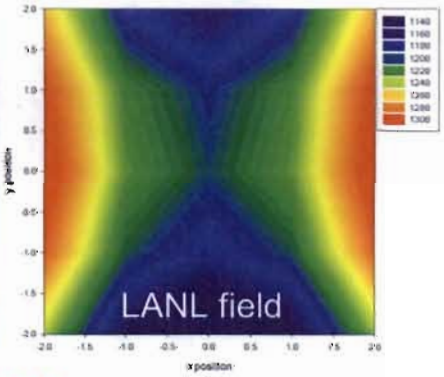

LANL Magnets
Cu coils
15" diameter, 10.5" apart
~ 55 V, 19 A
1200 Gauss, 0.12 T

Gauge designs at LANL

John Vorthman & Jerry Wackerle (early 1980's)

Designed and Constructed Magnet for Gun
Designed and Learned how to Make Gauges
Both Impulse & Velocity Gauges

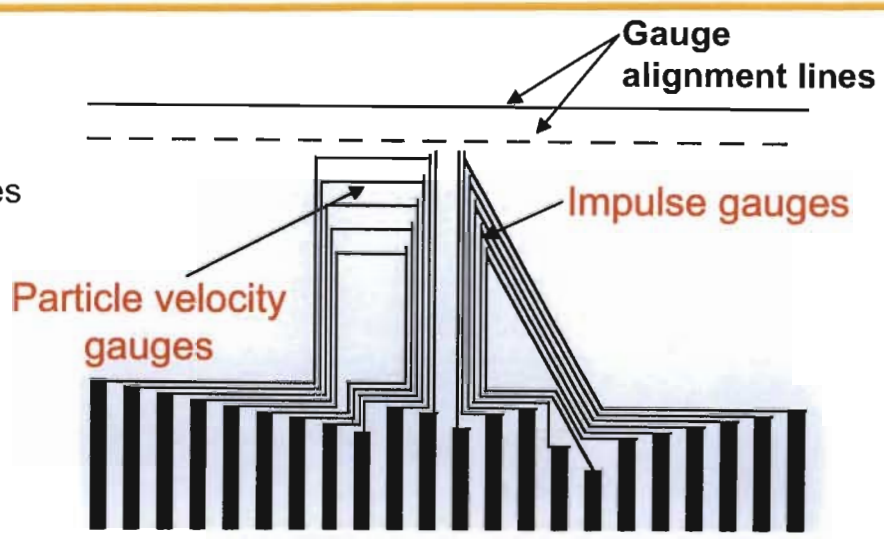

Steve Sheffield & Rick Gustavsen (late 1980's)

Staggered particle velocity gauges (10)
Center shock tracker
Sandwich – FEP Teflon, alum, FEP Teflon

(25 μm, 5 μm, 25 μm = 55 μm total)

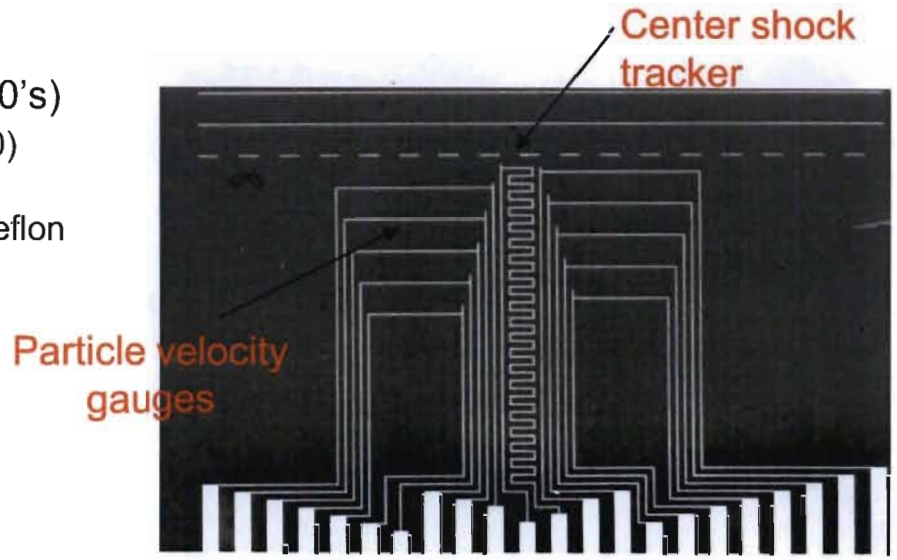

Modern gauge package at LANL

Steve Sheffield & Rick Gustavsen (1990s)

9 particle velocity gauges
3 shock trackers
Sandwich – FEP Teflon, alum, FEP Teflon

(25 μm, 5 μm, 25 μm = 55 μm total)

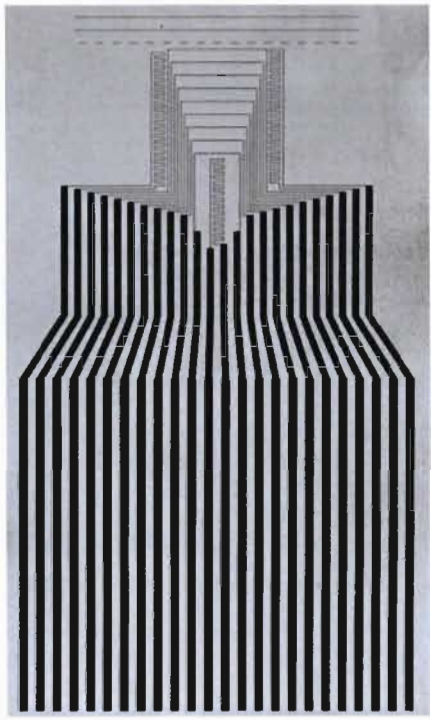

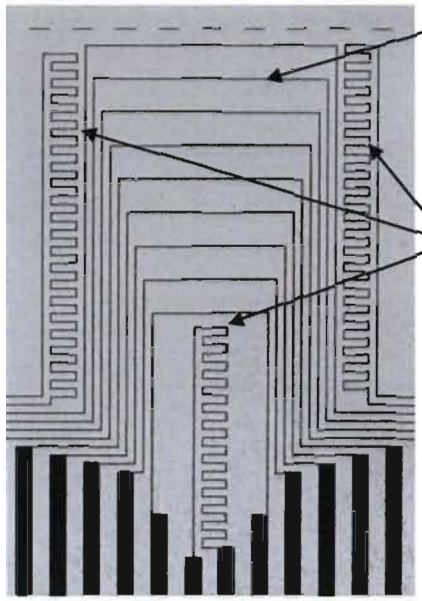

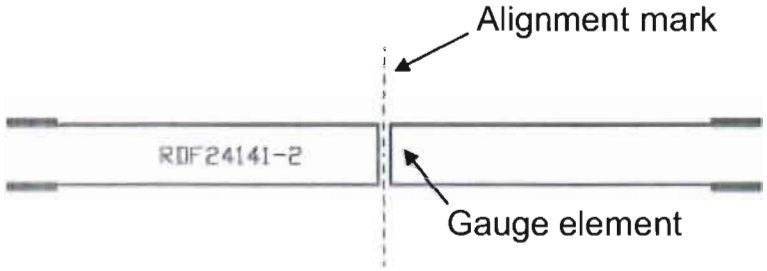

Stirrup gauge elements (25 μm thick)

Target preparation and alignment

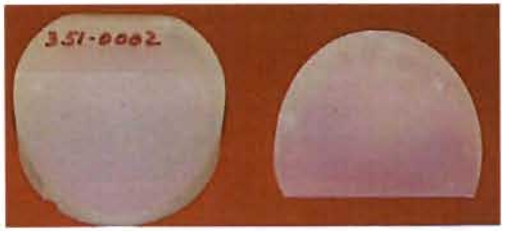

Typical target contains gauges at 30° angle

Insertion angle/position moves gauge elements relative to the front –
0.28 mm apart at 10° vs. ~0.8 mm at 30°

Tolerances – within 10 microns or less
Glue bonds – 1 to 5 microns

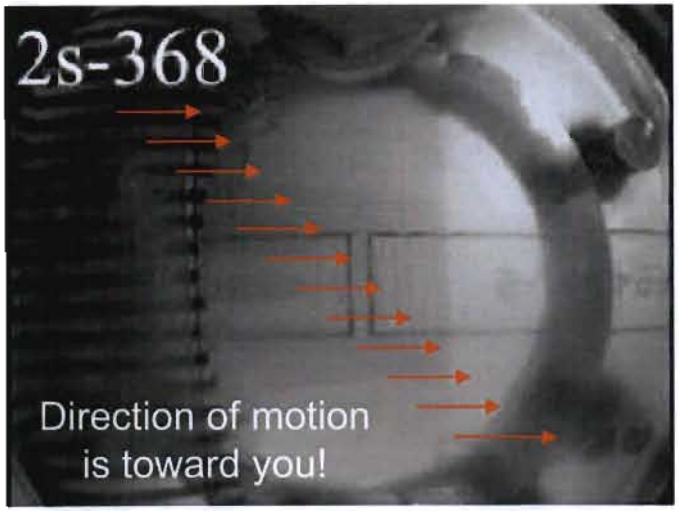

Rear view of transparent liquid target

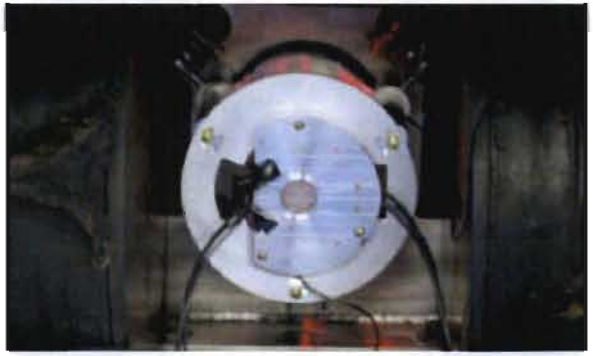

Target plate is scribed for alignment

UNCLASSIFIED

Target is then mounted to the end of the barrel in the uniform magnetic field.

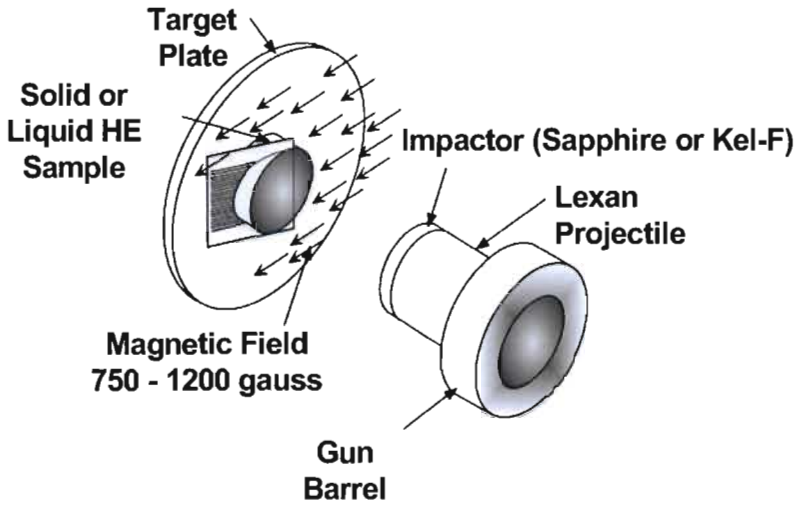

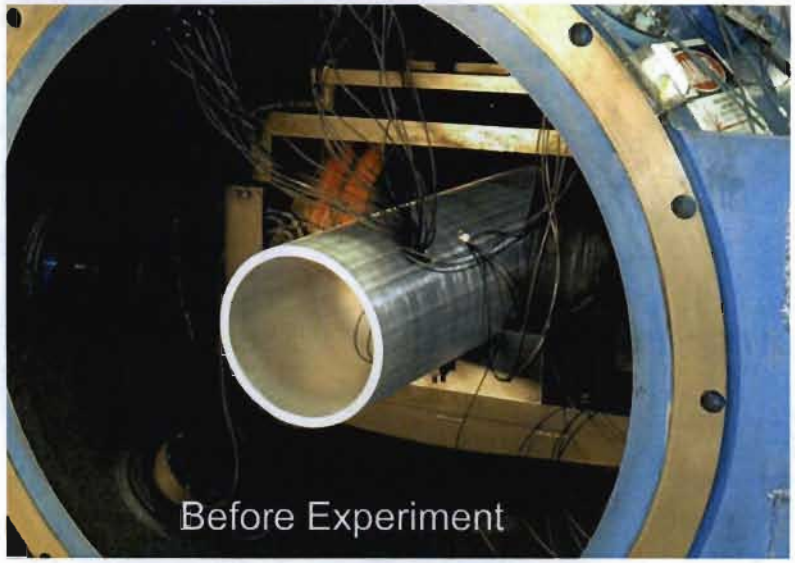

LANL two-stage gun

Gas breech driven - 15,000 psi

Projectile velocities- 1.2 to 3.6 km/s

Pump Tube/Launch Tube - 100/50 mm dia.

LANL single-stage gun

Gas breech driven – WAB, DD

Projectile velocities- <100 m/s to 1.5 km/s

Launch Tube - 78 mm dia.

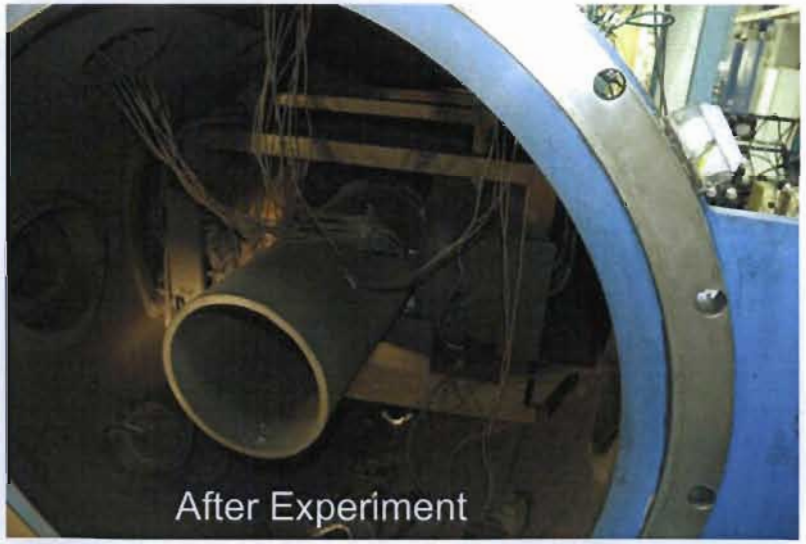

UNCLASSIFIED

We have extensively applied electromagnetic gauging to…

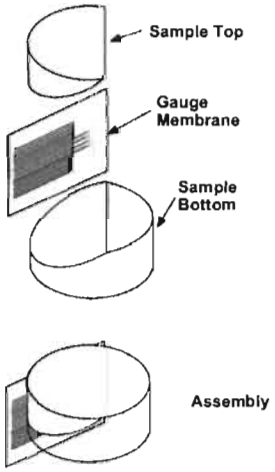

Solids

Solid explosives – PBX 9501, PBX 9502, TNT
Propellants – PBXN-9, HPP
Fluoropolymers, elastomers
Metallized polymers
(anything machinable)

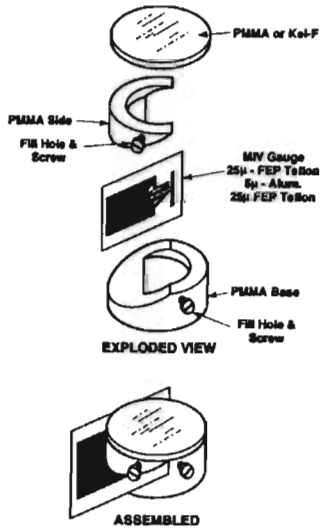

Liquids

Liquid explosives – NM, IPN, FEFO, H_2O_2
Liquid-particle mixtures
Organic liquids – phenylacetylene, benzene etc.
Gels – ballistic gelatin
(remote liquid loading system)

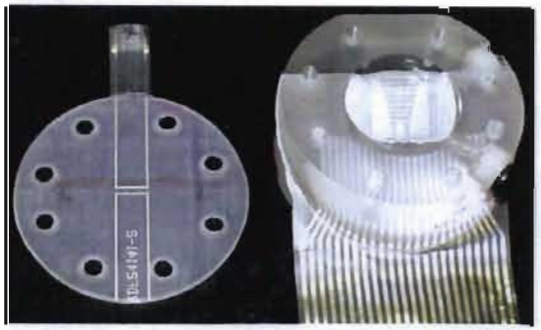

More complex samples…

Supported gauge package

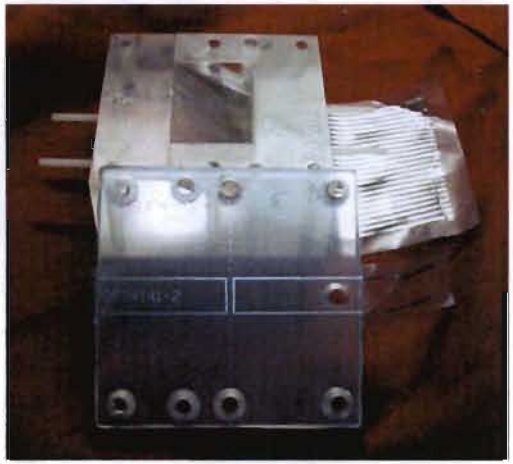

Powders, prills
Press-in-place
Gels

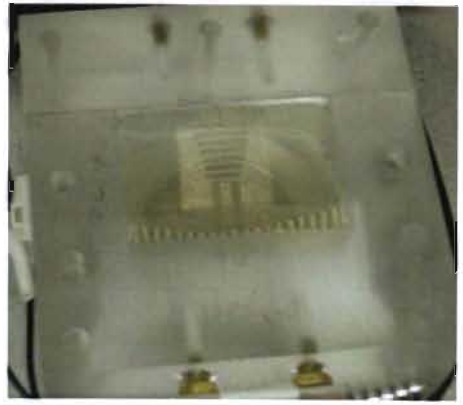

Layered stirrup gauges

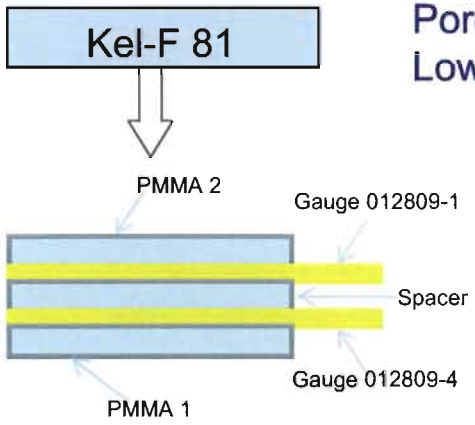

Thin samples (polymers)
Porous samples (HE, foams, powders)
Low density samples

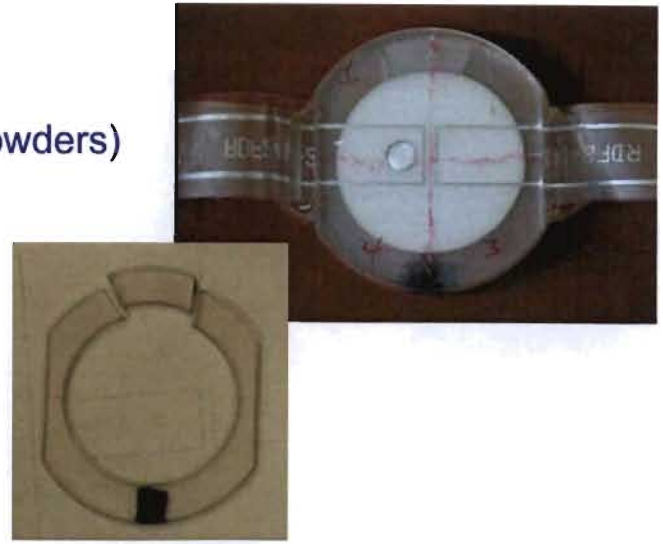

UNCLASSIFIED

Examples of shock wave profiles in an inert polymer (Kel-F 800)

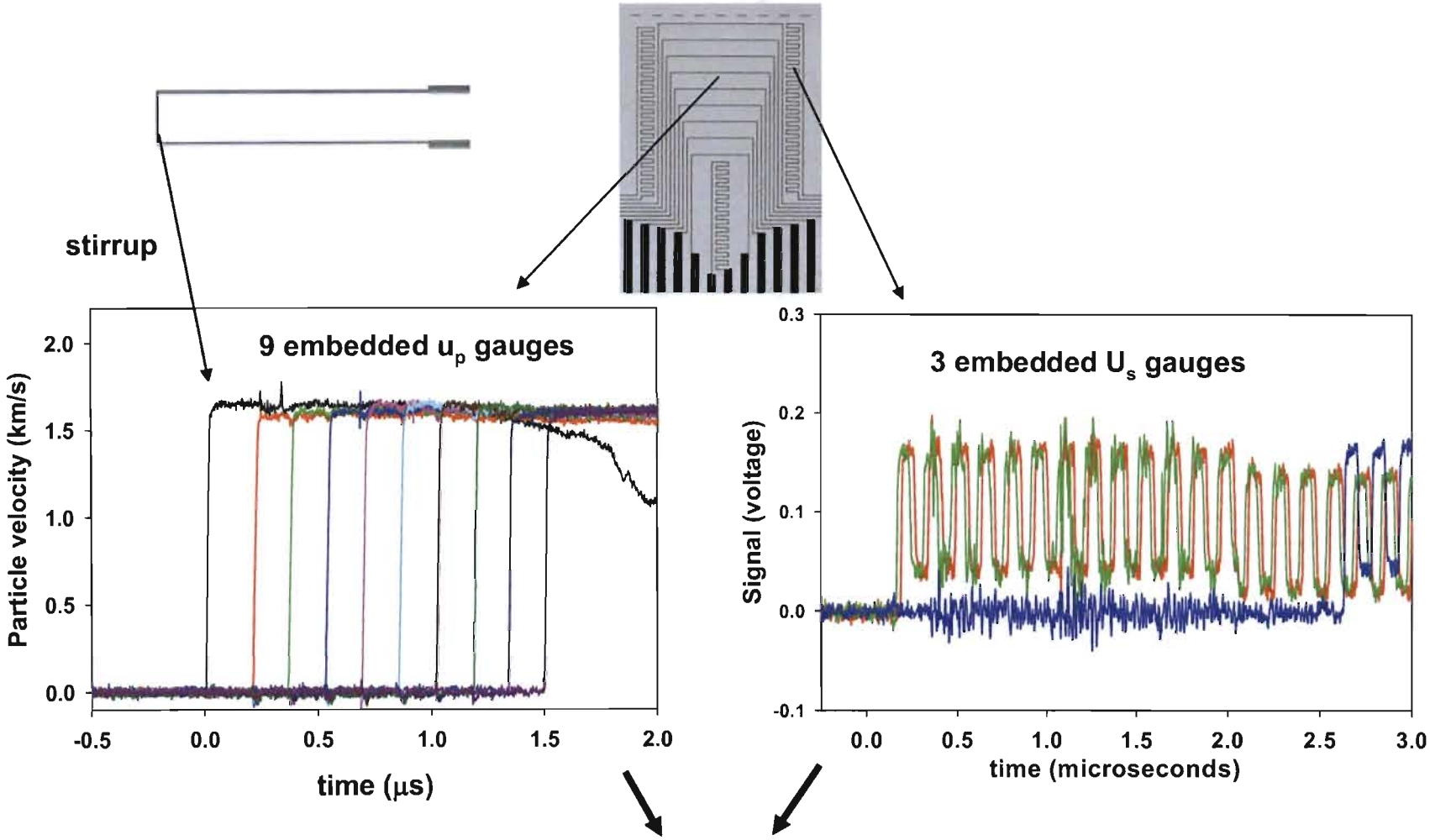

(U_s, u_p)

UNCLASSIFIED

Raw data analysis – particle velocity trackers

Raw recorded data

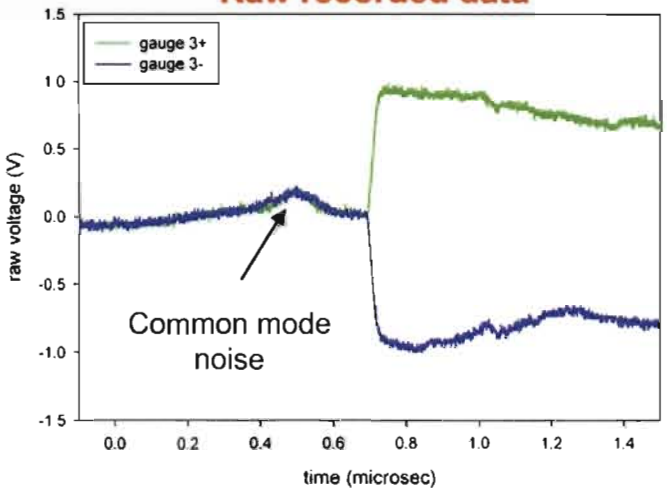

Example: heterogeneous initiation of NM/glass microballoon solution

Conversion to u_p

Voltage → particle velocity

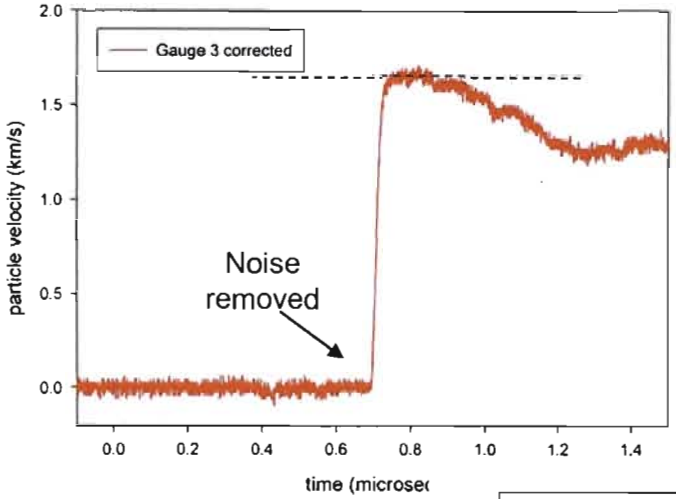

Voltage data for each gauge is subtracted, converted, & corrected in time

$$V = B \times L \times u_p$$

$$F = \frac{(1 + \frac{R_g(\Omega)}{R_s(\Omega)})}{B \times L}$$

Final Data

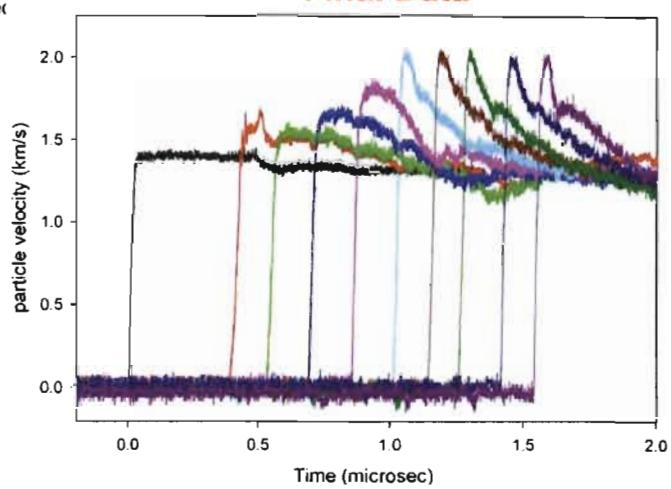

Shock input determined from initial u_p

Field is measured before each shot
Time correction accomplished using fiducial pulse

UNCLASSIFIED

Reduction of shock tracker data gives high fidelity determination of shock, detonation velocities, and time to detonation.

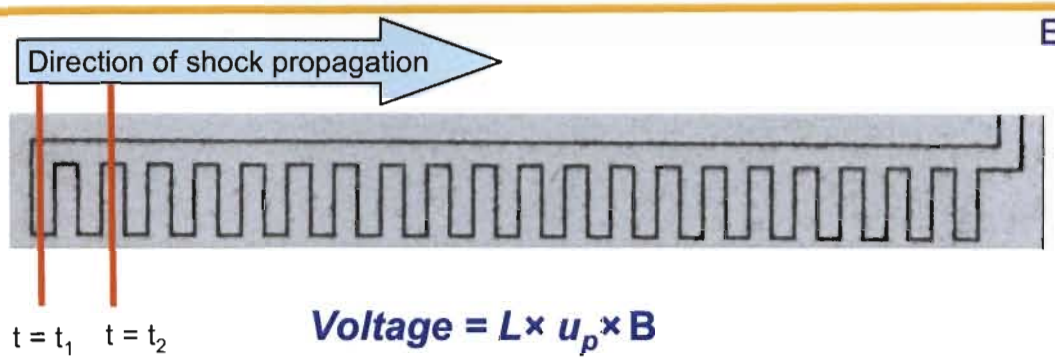

Example: heterogeneous initiation of NM/glass microballoon solution

$$Voltage = L \times u_p \times B$$

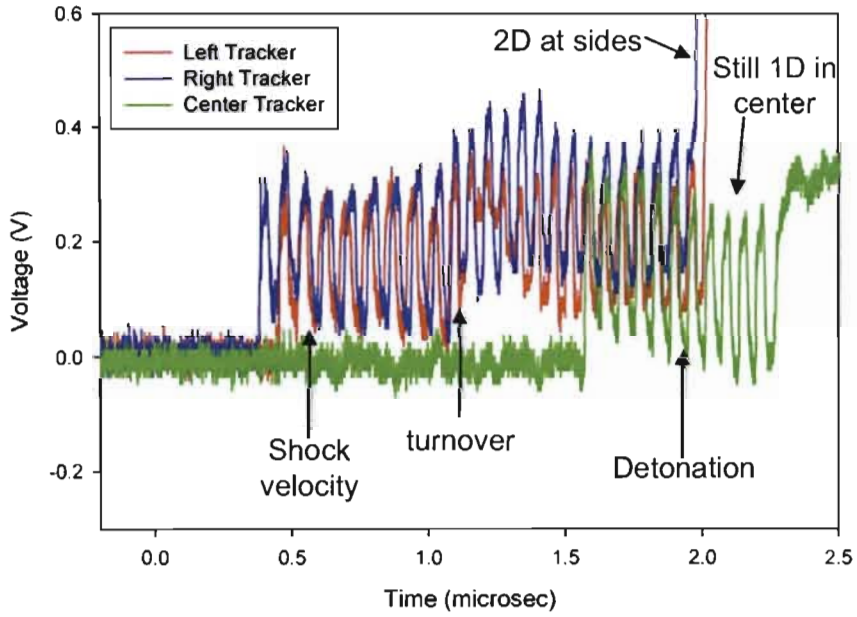

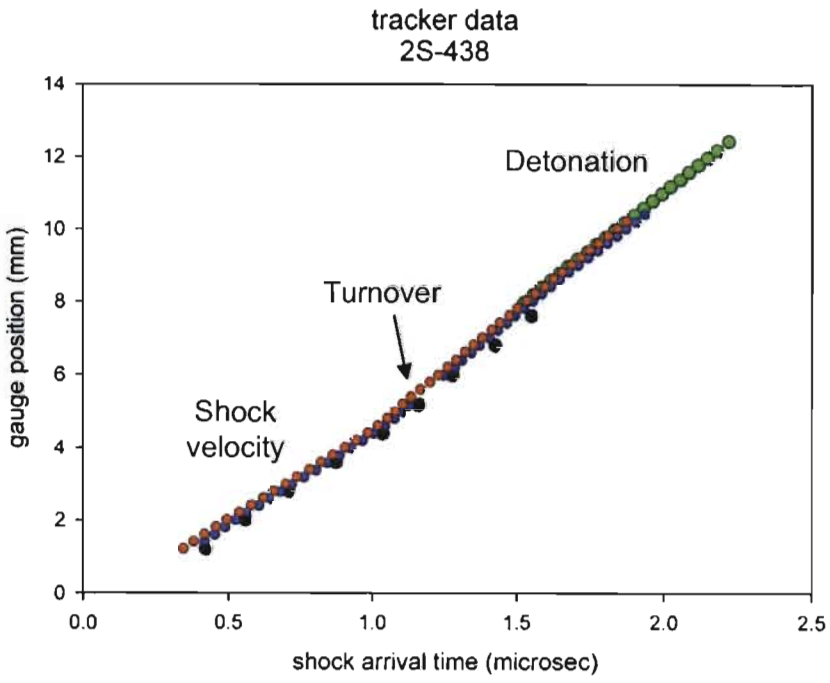

Data interpretation

- When the experiment is over – 2D effects, gauge breaking
- Limitations of temporal resolution
- Error
  - Sample preparation
  - Experimental conditions
- Impedance mismatches (including air gaps)
- Viscoelasticity

UNCLASSIFIED

Temporal resolution is ~ 10-20 ns – clips vN spike on detonation wave

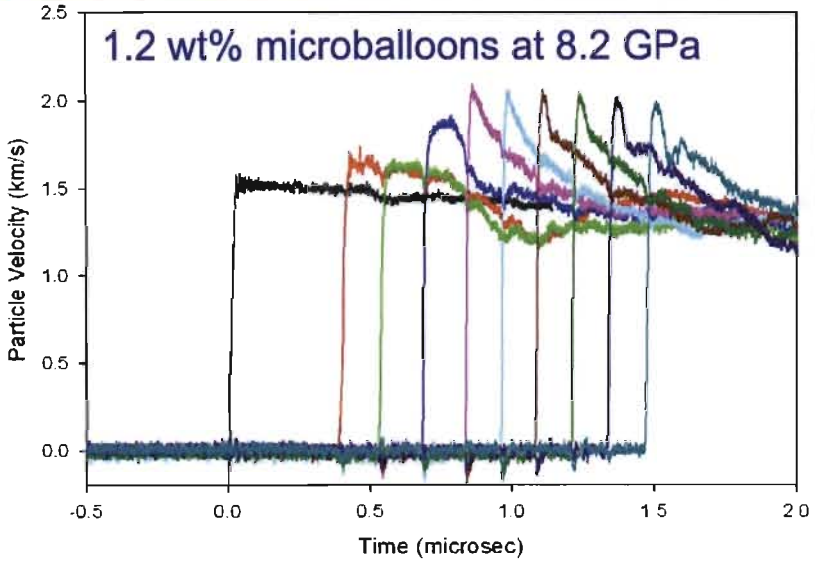

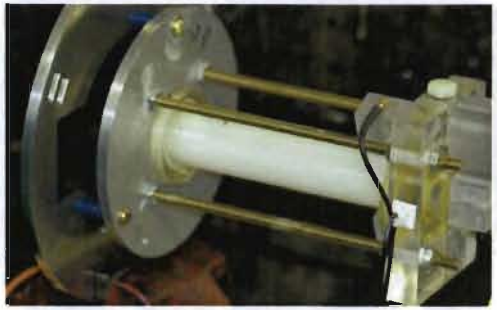

- vN spike by VISAR – 2.2 km/s
- vN spike by gauges – 2.1 km/s

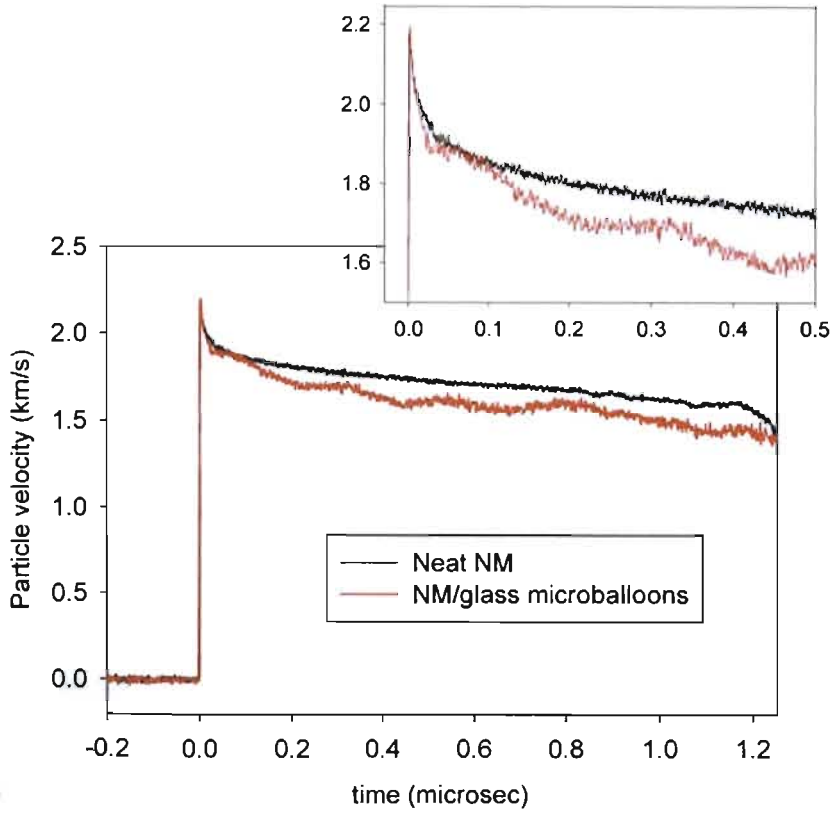

UNCL

Error analysis

- Numerous experiments – validation of gauge data against VISAR/PDV (good check)
- Error is ~1-2% (both U_s and u_p) – multiple fits to x-t data, u_p from profiles
- Sources of error:
  - Sample preparation
    - Leg deflections up to 16° resulted no effect
    - Gauge length readings (within 1%)
    - Thick glue bonds lead to ramped waves
    - Gauge "roll" leads to ramped waves, noise

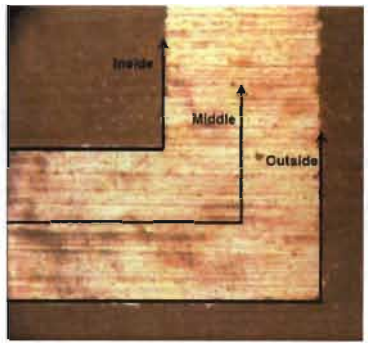

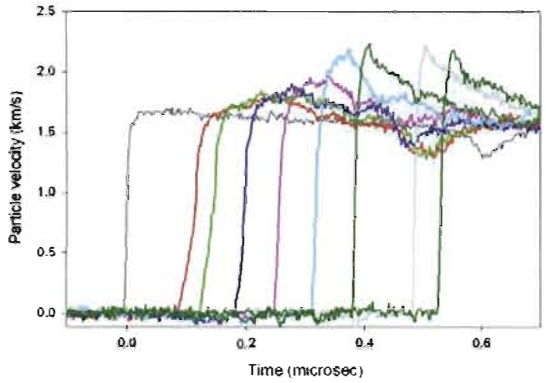

  - Alignment and tilt, experiment
    - Tilt and misalignment result in < 1% error
      - Example: 100 mrad tilt (large, typ. 3 mrad) ~ 1.1% error in u_p
    - Lead spreading (gauge stretching) – results in increase in u_p, gauge protection

UNCLASSIFIED

Inclined gauges in liquids – gauge/liquid impedance mismatches

- Gauges are good impedance match to solid explosives (no issues to date)
- Stirrup gauge reads correct input shock, embedded gauges may read higher/lower
- Results in uncertainties in the particle velocities of evolving waves

Lower Impedance
Velocity Lower

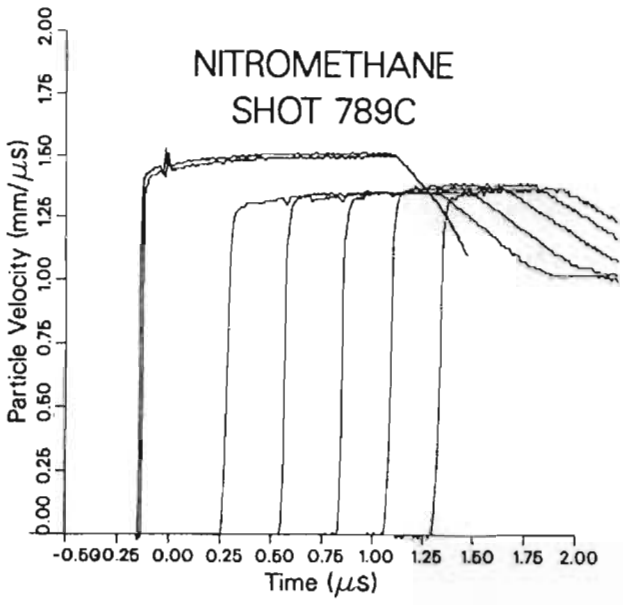

Higher Impedance
Velocity Higher

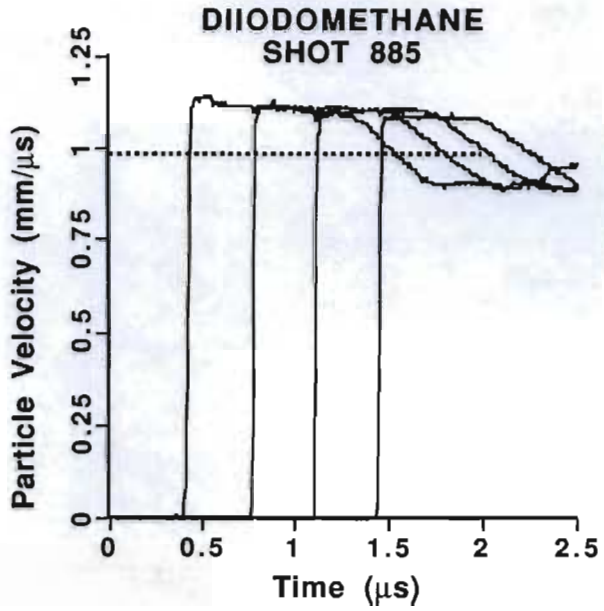

Impedance over-/under-match depends on angle of gauge insertion

Gauge Angle	NM Undermatch	Liquid CH_3Br Match	CH_2I_2 Overmatch
0°	± 2 %	-------	-------
10°	- 2 to 4 %	-------	+ 1 to 2 %
20°	-5 to 6 %	-------	+ 3 to 4 %
30°	- 8 to 10 %	± 2 %	+9 to 10 %

Easily Checked Using a Stirrup Gauge at Input to Liquid

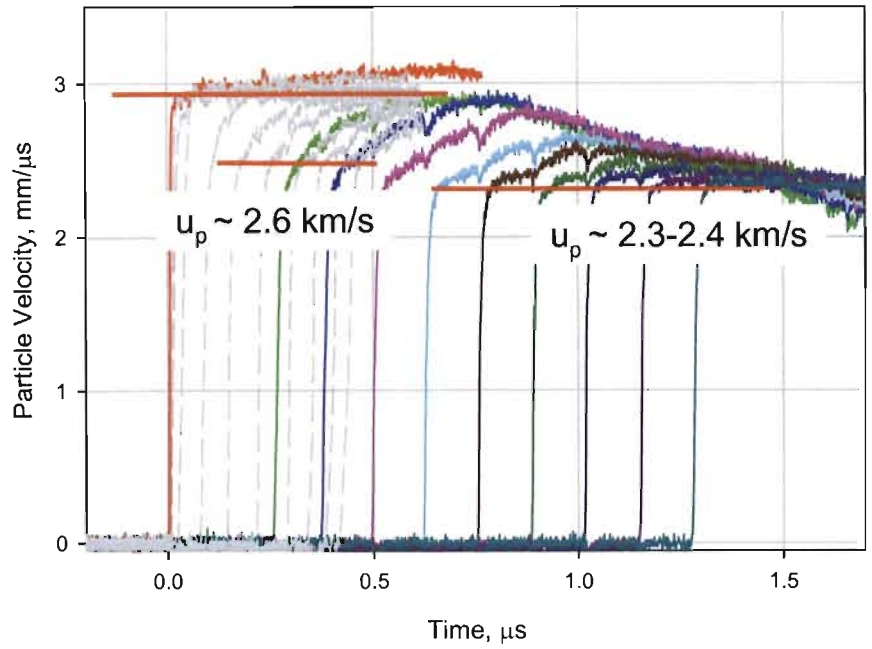

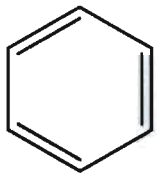

benzene
Boiling point – 80.1 °C
Density – 0.877 g/cm³
Sound Speed – 1.31 mm/μs

Example data of benzene:
Same input with gauges at 10° and 30°

Input is well-defined by stirrup gauge
First wave u_p is influenced by mismatch

Air gaps = jump in u_p - examples

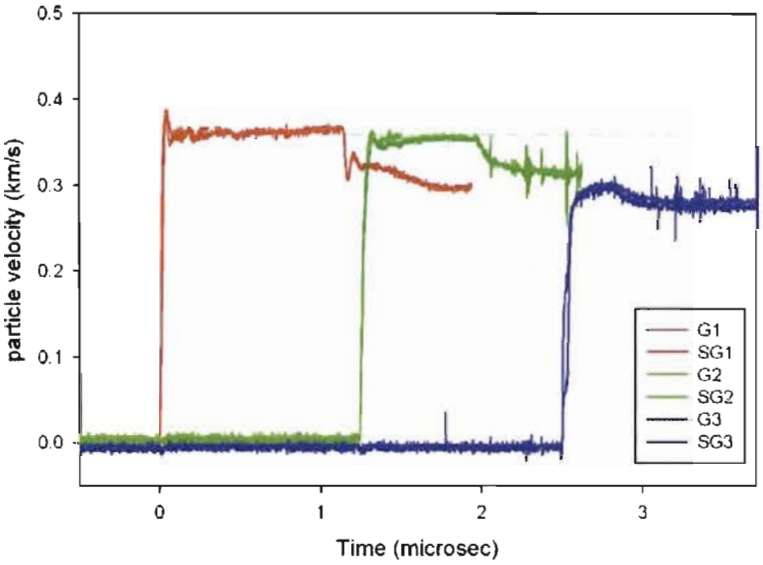

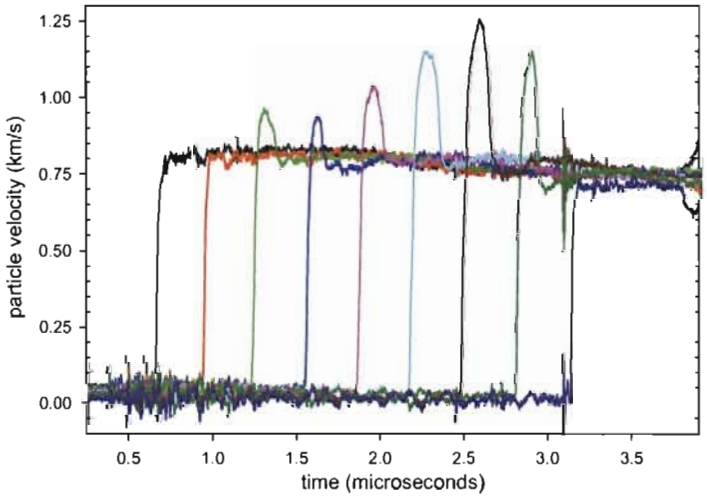

Layered target of rubbers

Small spike on first gauge - gap

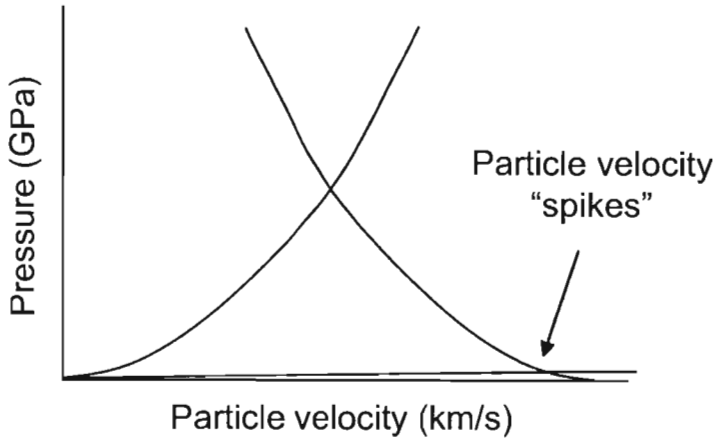

Embedded gauge exp't on ballistic gelatin

Gelatin pulled away from embedded gauge

mm-sized gap closed by shock

Low velocity impact into polymers results in viscoelasticity observed in profiles.

Symmetric Impact of PMMA
(Barker and Hollenback, 1970)
(Schuler and Nunziato, 1973-5)

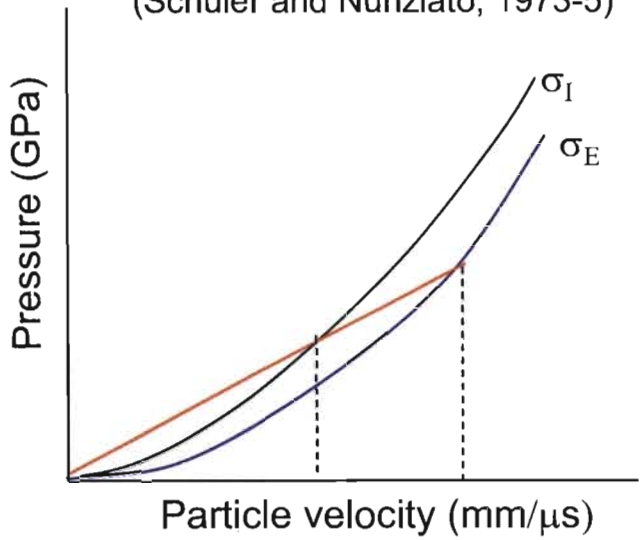

Wave evolves over time/distance
Rounding is more pronounced at low pressures

From shock wave profiles, we can construct instantaneous and equilibrium Hugoniots

Example: Kel-F 800

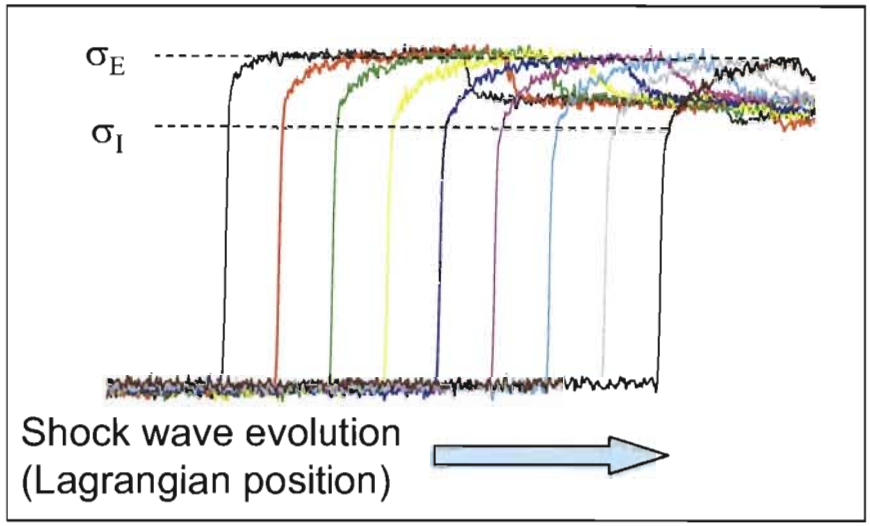

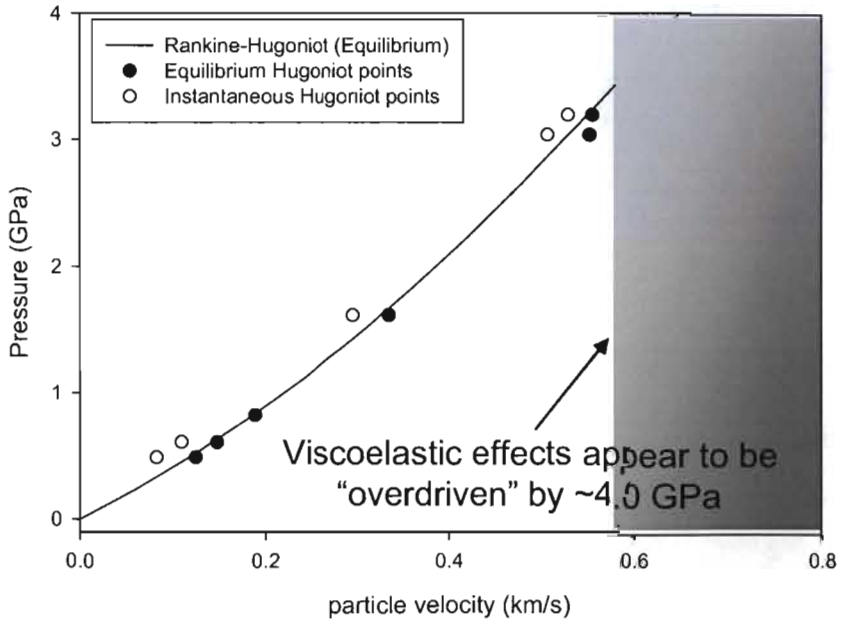

Research Examples

- In-situ magnetic gauging is best means of studying wave evolution
- Where would we observe wave evolution (mechanical variables)?
    - phase transitions, melting, chemistry
- Shock-to-detonation transition (initiation) in explosives
    - general introduction to shock initiation
    - role of hot spots
- Shock-induced chemical reactions

UNCLASSIFIED

In-situ gauging has significantly improved our understanding of the shock initiation of explosives.

- Development of "Pop-plots"- shock input pressure vs. run distance (time) to detonation
  - Wedge tests, small and large scale gap tests nearly obsolete in DOE
- Definition of shock initiation mechanisms – solid explosives, liquid explosives
  - Hot spot driven vs. thermal explosion driven mechanisms
- High fidelity comparison experiments – effects of density, lot, temperature, aging
- Complex loading – short shock, double shock etc.
- Data for parameterization of modern reactive burn models –

  Ignition and Growth, CREST, etc.

UNCLASSIFIED

Different types of explosive materials have different initiation behaviors.

Homogeneous Explosives

HMX, PETN, RDX single crystals (L to R)

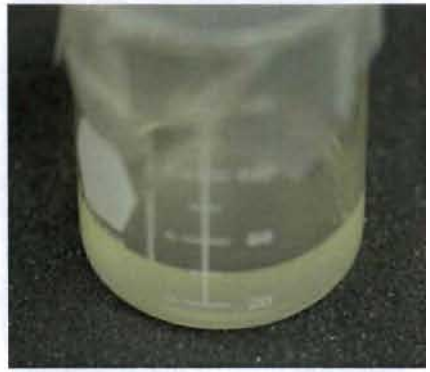

Liquid explosives:
nitromethane,
hydrogen peroxide,
isopropyl nitrate, etc.

Heterogeneous Explosives

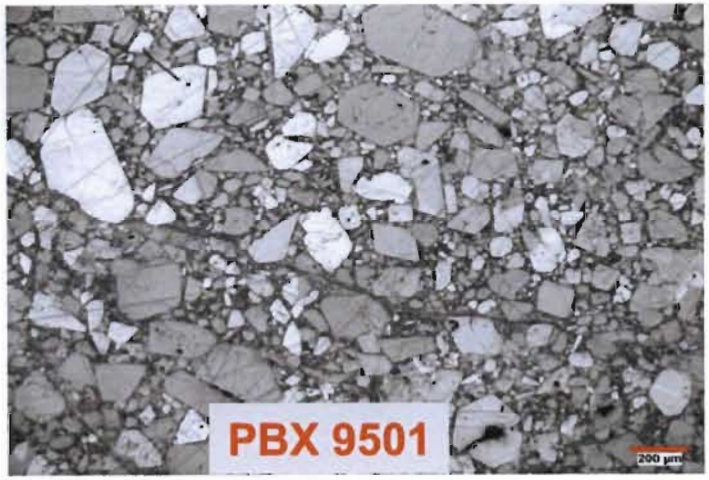

Most explosives are "heterogeneous" with complex microstructures.

PBX 9501

95/2.5/2.5 HMX/Estane 5703 binder/NP
Bimodal distribution of explosive grains
2-3% porosity; Many impedance mismatches

Single crystals grown by D. Hooks; PBX micrograph by Paul Peterson

Heterogeneous explosives initiate by localization of energy in “hot spots.”

- Hot spots – localized high P/T due to microstructures
- Reactive growth occurs in or near the shock front
- Acceleration of wave, shock velocity-detonation velocity
- Detonation is nearly steady at overtake

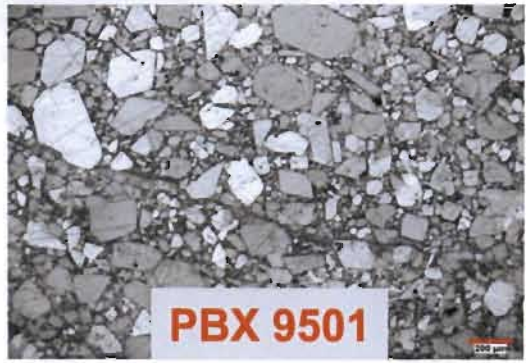

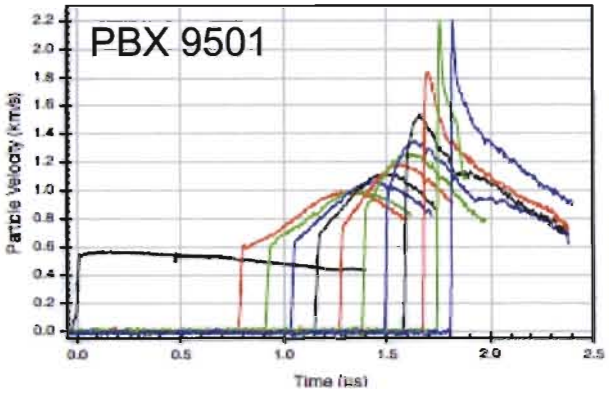

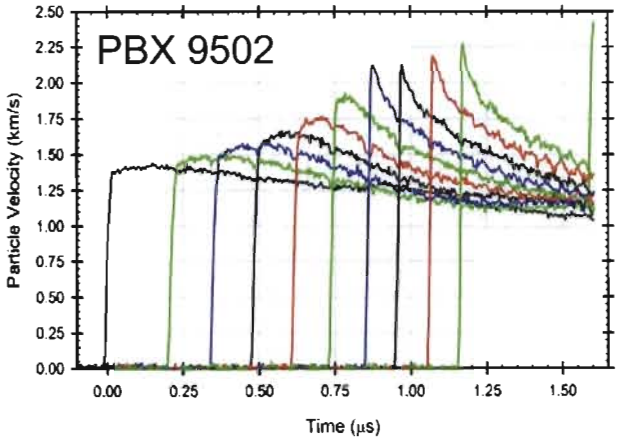

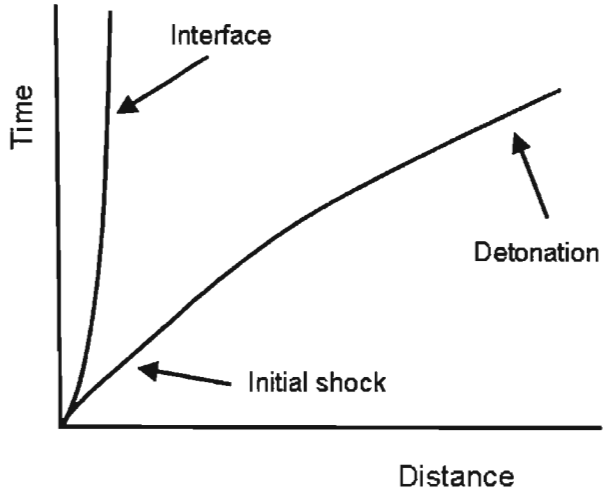

UNCLASSIFIED

In-situ gauging allowed for refinement of homogeneous initiation model.

Campbell, Davis, & Travis (Chaiken)

Campbell, Davis and Travis (1961)
Chaiken (1958, 1960)

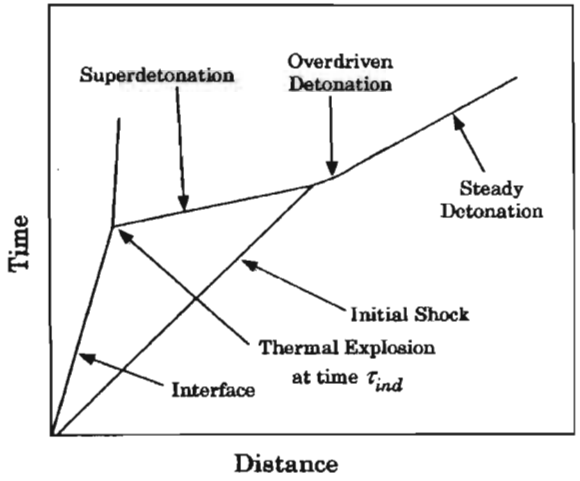

Sheffield, Engelke, & Alcon

Sheffield and Alcon (1989)

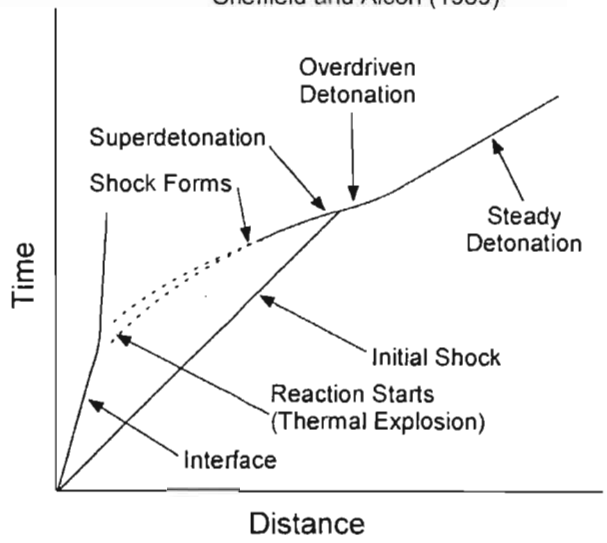

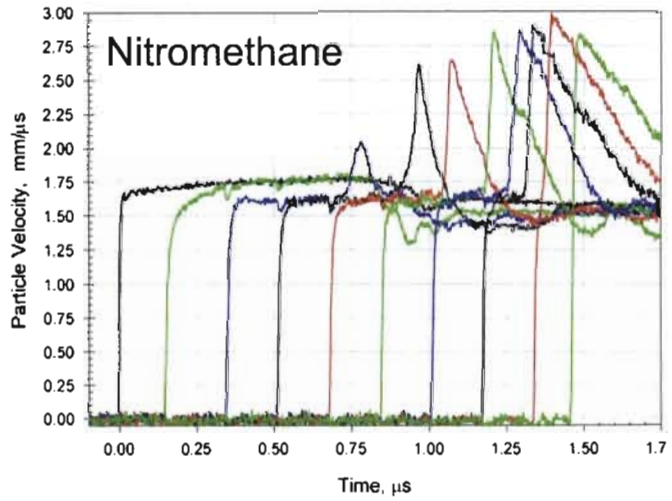

- "Bulk" sample must be shock heated
- Thermal explosion occurs after induction time
- Reactive wave forms, travels behind the front
- May grow to superdetonation
- Detonation is overdriven at over-take

$$\tau = \frac{C_v R T^2}{AQE} e^{E_a / RT} \qquad \frac{dt}{t} = -21.7\left(\frac{dT_0}{T_0}\right)$$

UNCLASSIFIED

Nitromethane-particle mixtures serve as a tractable system for probing hot spot physics.

- Goal of this work is to interrogate the influence of well-defined hot spot features (impedance mismatches and voids) on ***shock initiation.***

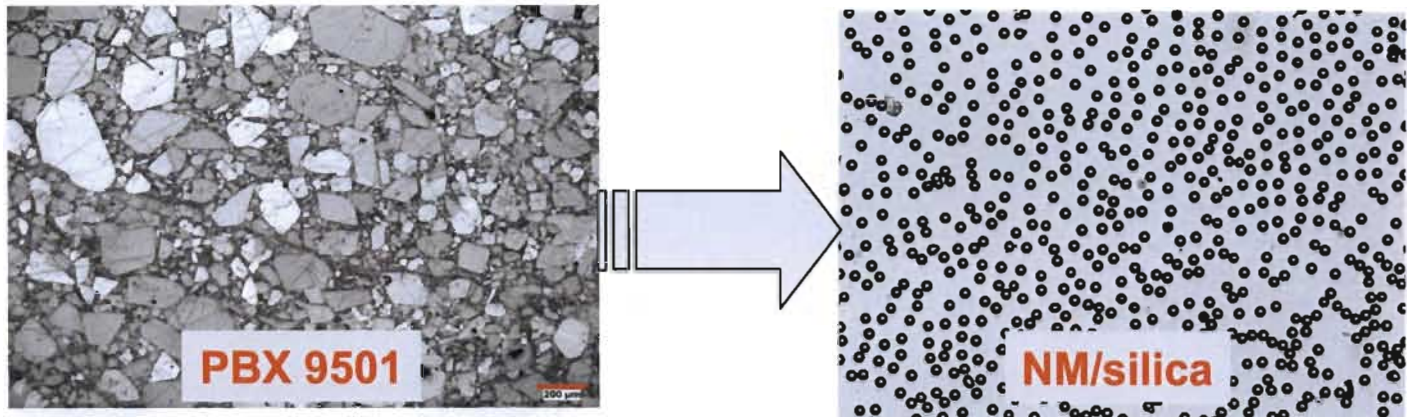

95/2.5/2.5 HMX/Estane 5703 binder/NP
Bimodal HE grain distribution; 2-3% porosity

Nitromethane/6 wt% 40μm silica

- Solutions of NM gelled with Guar
- Solid glass beads as shock impedance mismatches
- Hollow glass microballoons as porosity
- Measure in-situ flow associated with build-up to detonation
- Pop-plots – shock initiation thresholds

P.D. Peterson, PBX 9501 micrograph

UNCLASSIFIED

Nitromethane is well characterized and has been shown to be "sensitized" by both physical and chemical additives.

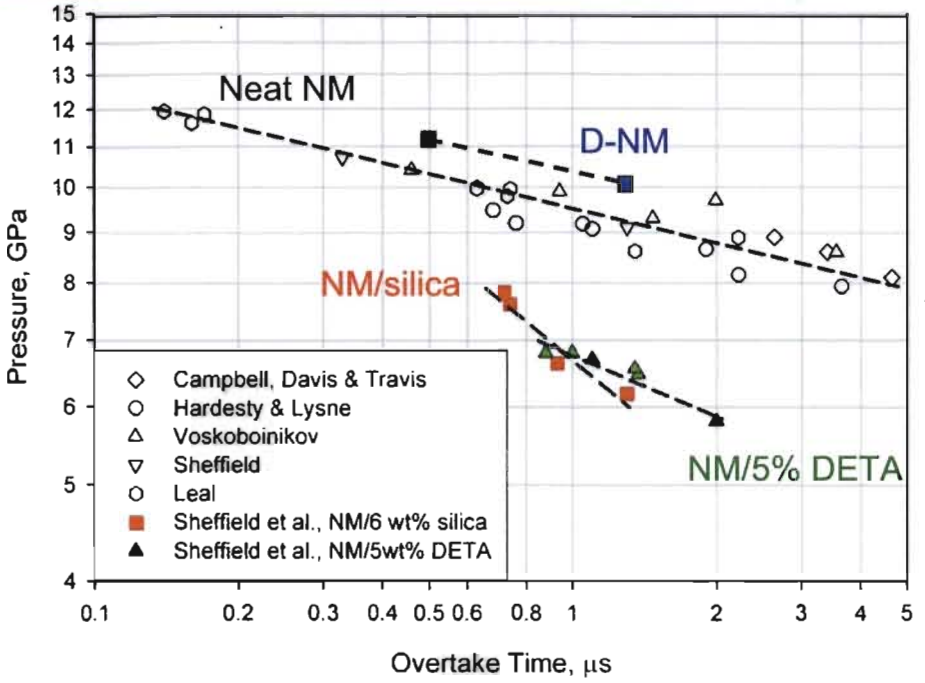

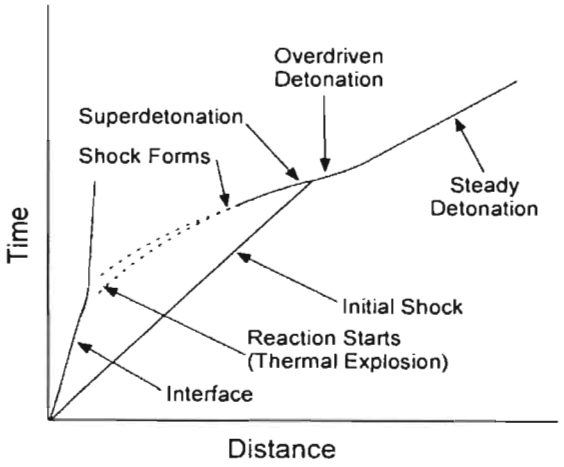

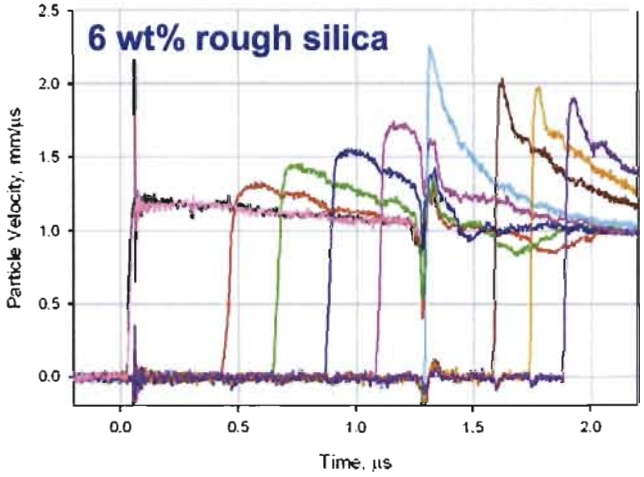

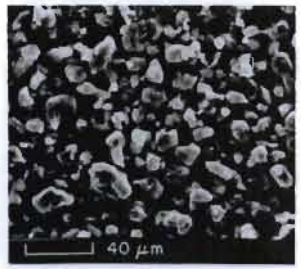

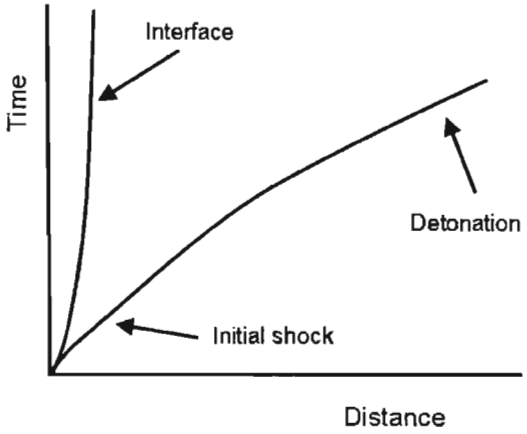

UNCLASSIFIED

Fabrication and characterization of explosive samples is essential to interpreting hot spot effects.

- Gelled with guar at 1.75 – 1.85 wt%

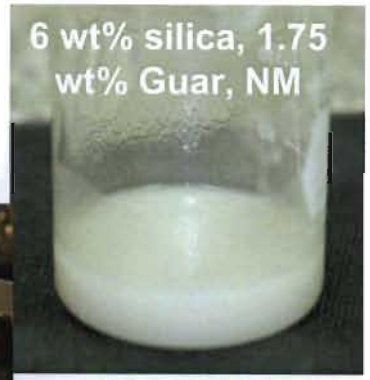

Solid beads

- 1-4 and 40 μm diameter silica
- Studied at 6 wt% (2.8 vol%)

ρ_{bead} = 2.45 g/cm^3

- L_p = 6 and 106 μm

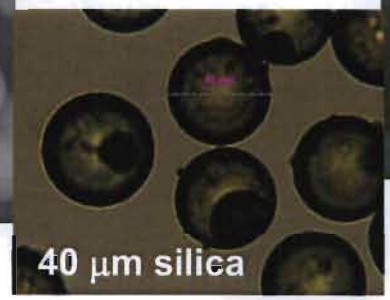

Hollow microballoons

- Sieved to avg. diam. ~ 42 μm
- 38.3-45.8 μm range

$\rho_{balloon}$ = 0.46 g/cm^3

- 1.2 and 0.36 wt% (2.8, 0.84 vol%)
- L_p = 106 and 158 μm

- Wall thickness ~ 0.8 μm
- Fraction of glass ~ 12%

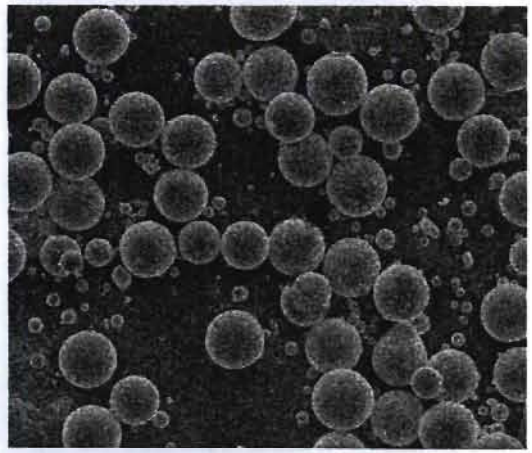

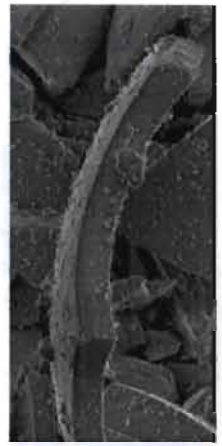

B. Patterson, LANL, SEM micrographs

UNCLASSIFIED

Controlled, tractable heterogeneities – *glass beads as impedance mismatch*

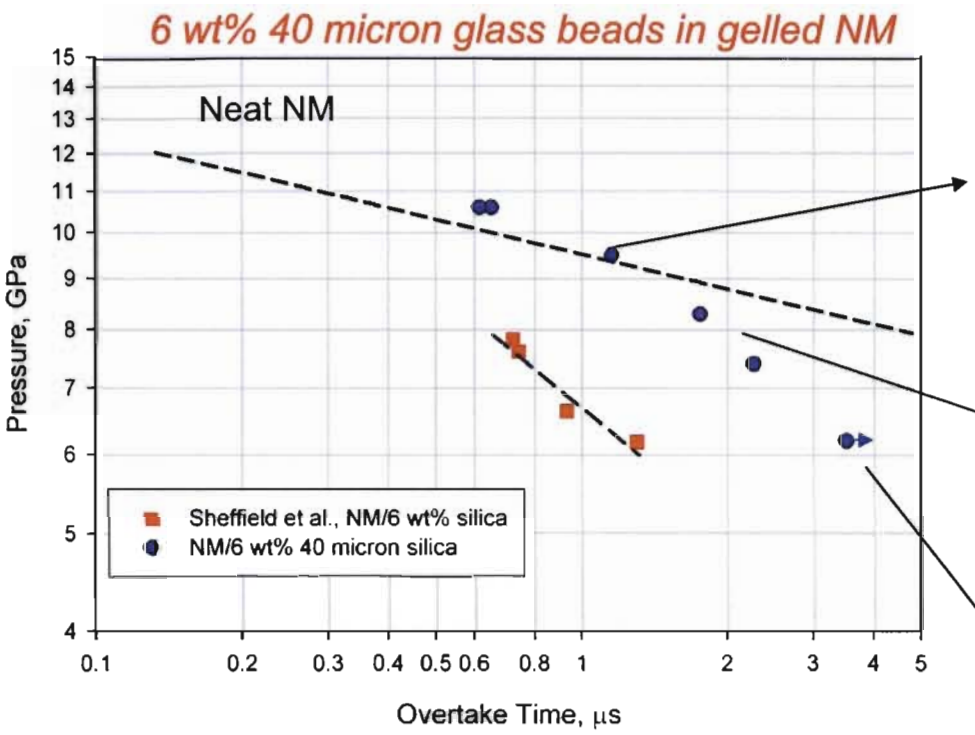

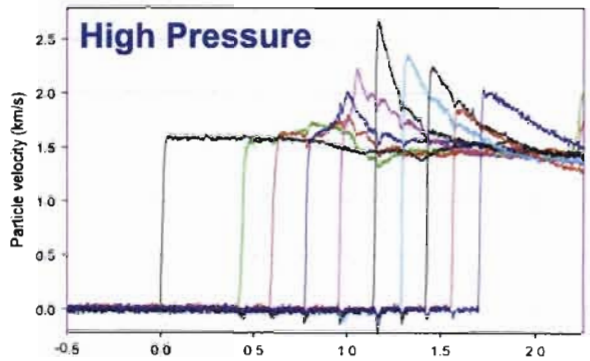

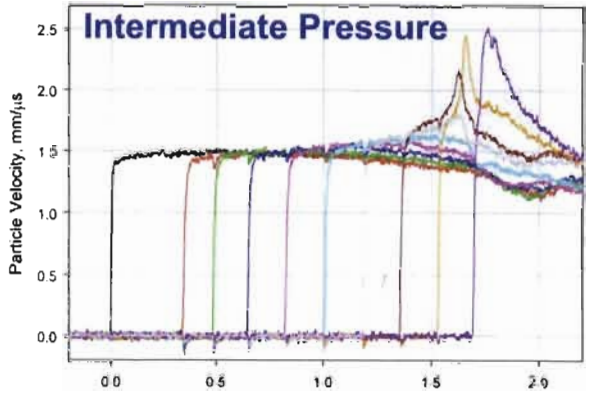

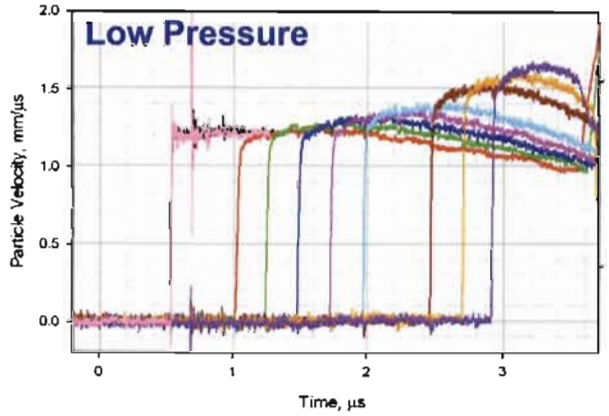

- Beads are ~ 106 μm (2.5 diameters) apart
- Build-up process is highly shock input pressure-dependent
- Pop-plot is non-linear

UNCLASSIFIED

Small beads at a higher volumetric concentration produce more effective hot spots.

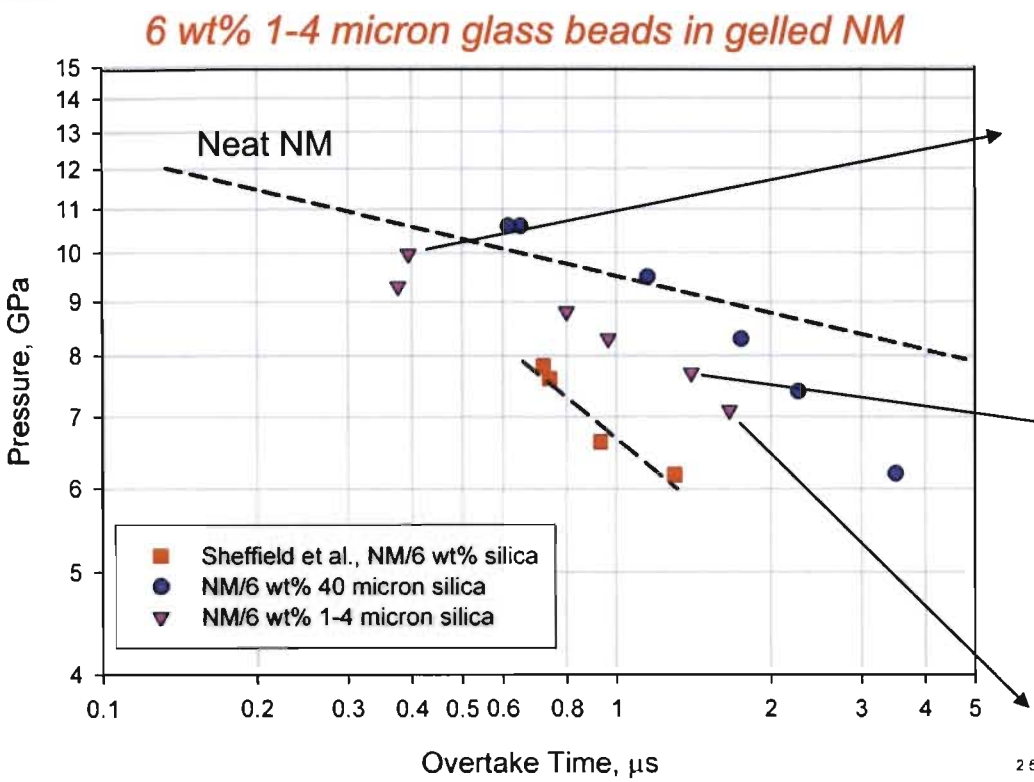

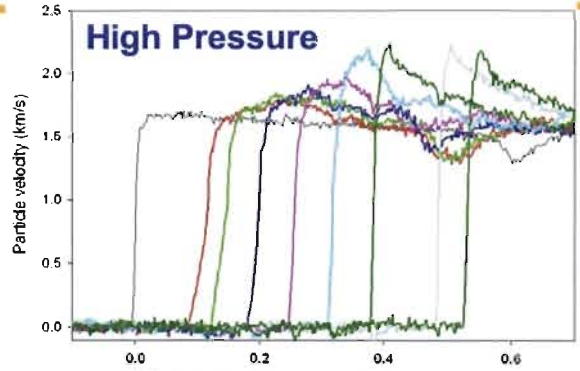

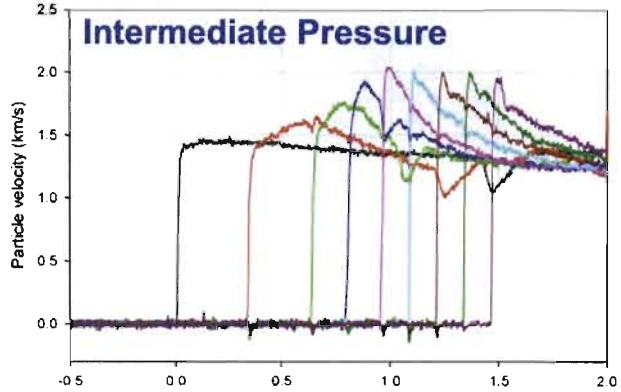

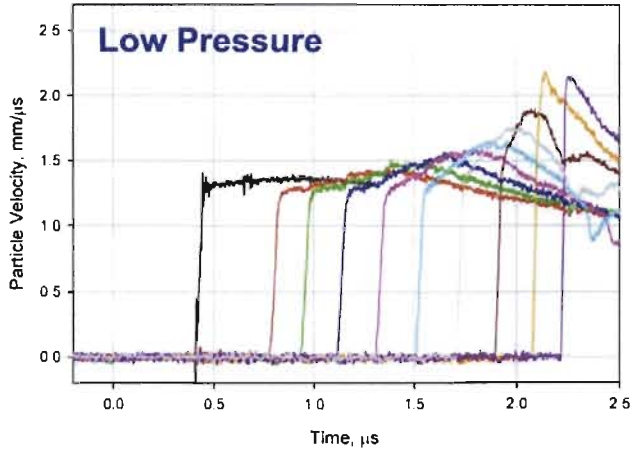

- Beads are ~ 6 μm apart
- All shock inputs result in "heterogeneous-like" build-up behavior
- Reactive flow shows some dependence on input shock strength

Hydrodynamic collapse of voids might be expected to produce a higher volumetric concentration of hot spots.

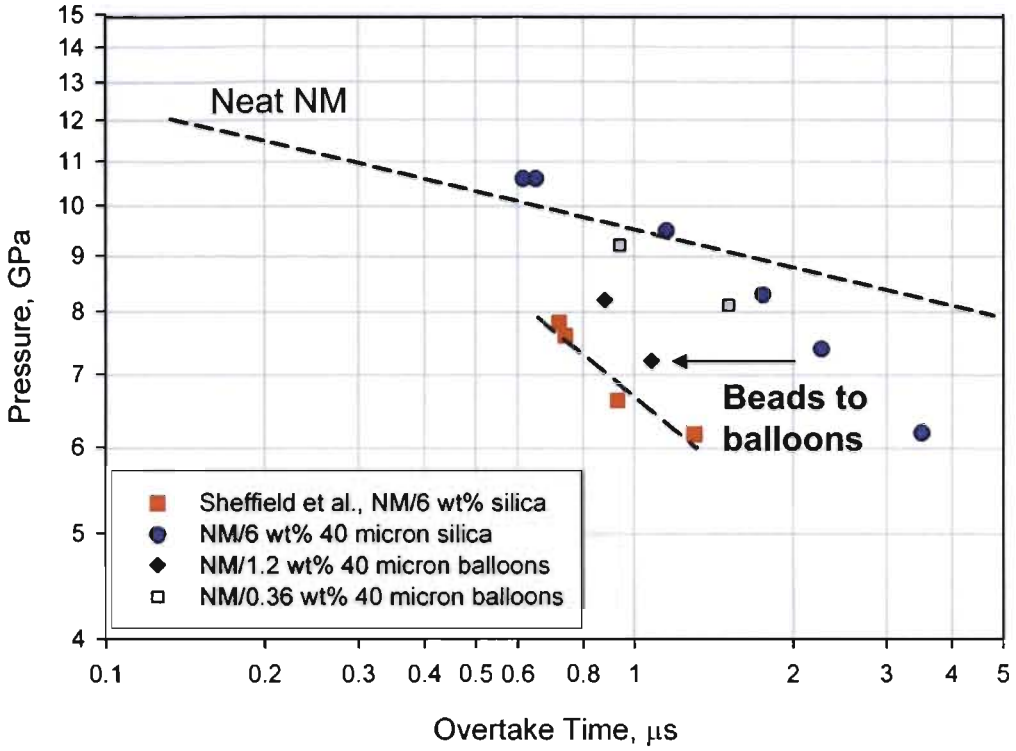

xRAGE simulation of 10 GPa shock traversing 20 μm beads

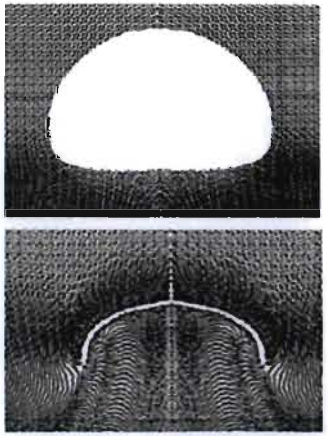

Hydrodynamic collapse expected to produce hot spot at each balloon

- Microballoons at same volumetric loading and size as solid silica beads are significantly more sensitizing

R. Menikoff, LANL, NOBEL simulation of NM/silica
Mader, C. L. "Theoretical and Experimental Two-Dimensional Interactions of Shocks with Density Discontinuities", LA-3614, 1966.

Comparison of reactive build-up for voids spaced ~ 2.5 and 4 diameters apart

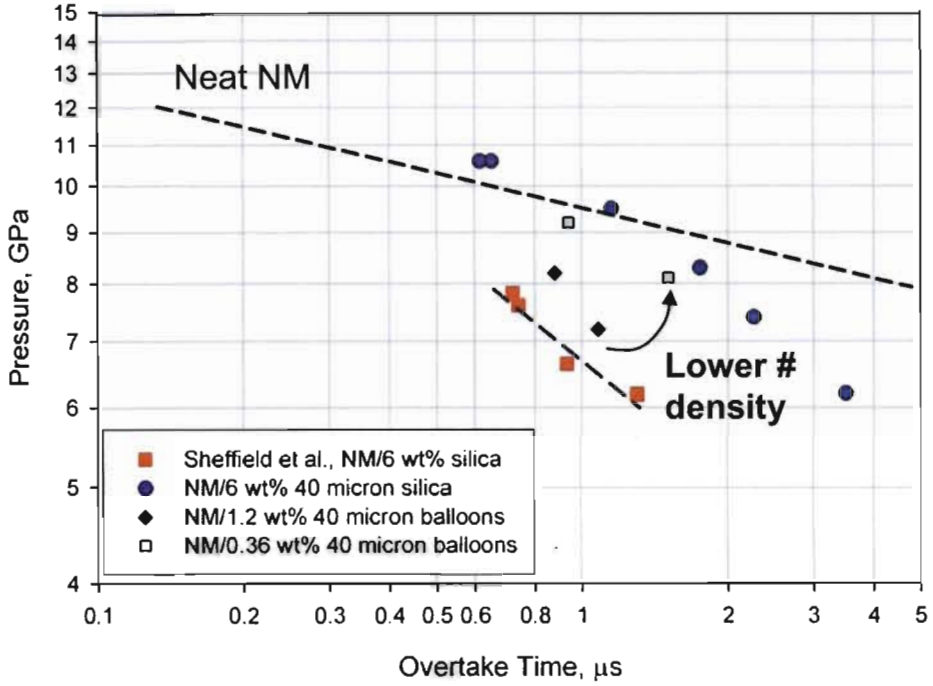

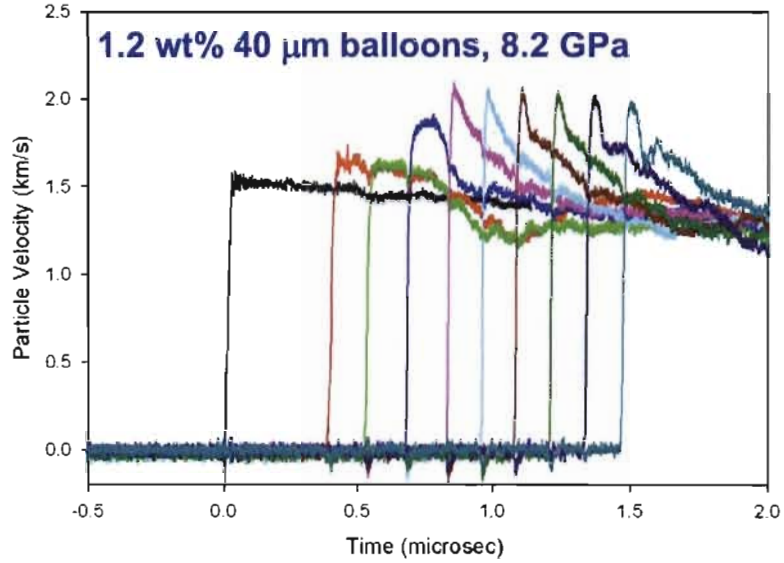

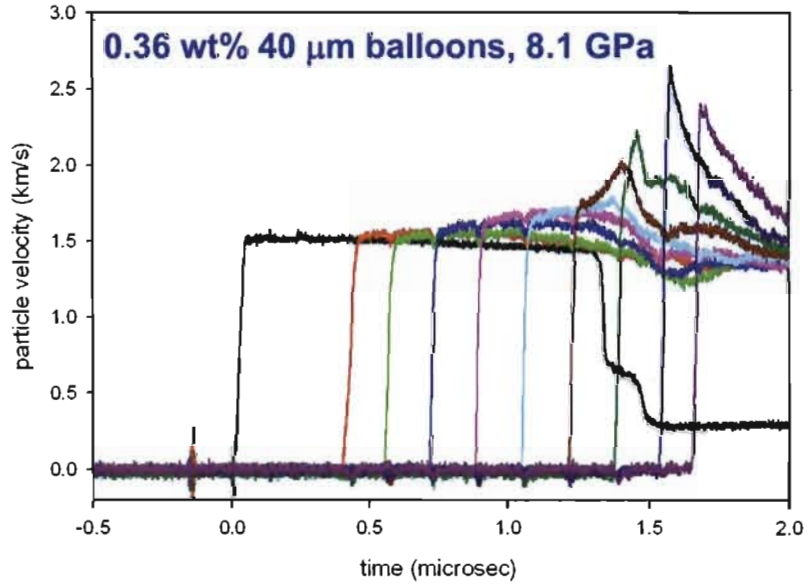

- Increasing inter-balloon spacing to 4 diameters moves Pop-plot toward neat NM data

- Build-up has characteristics of thermal explosion

There is a balance between hot spot- and thermal-driven shock initiation

Initiation behavior can be "tuned" by hot spots

1. Hot spot effectiveness:

- Porosity > impedance mismatches
- Multi-sized particles
- Small particles, closely spaced (L_p ~ few to 100 μm)
- Temp. ~ 50% higher than bulk

2. Hot spot criticality:

- Critical spacings in range 2.5- 4 diam.
- Pop-plot can be non-linear, returns to neat explosive
- Increasing shock input pressure decreases time available for hot spot coordination

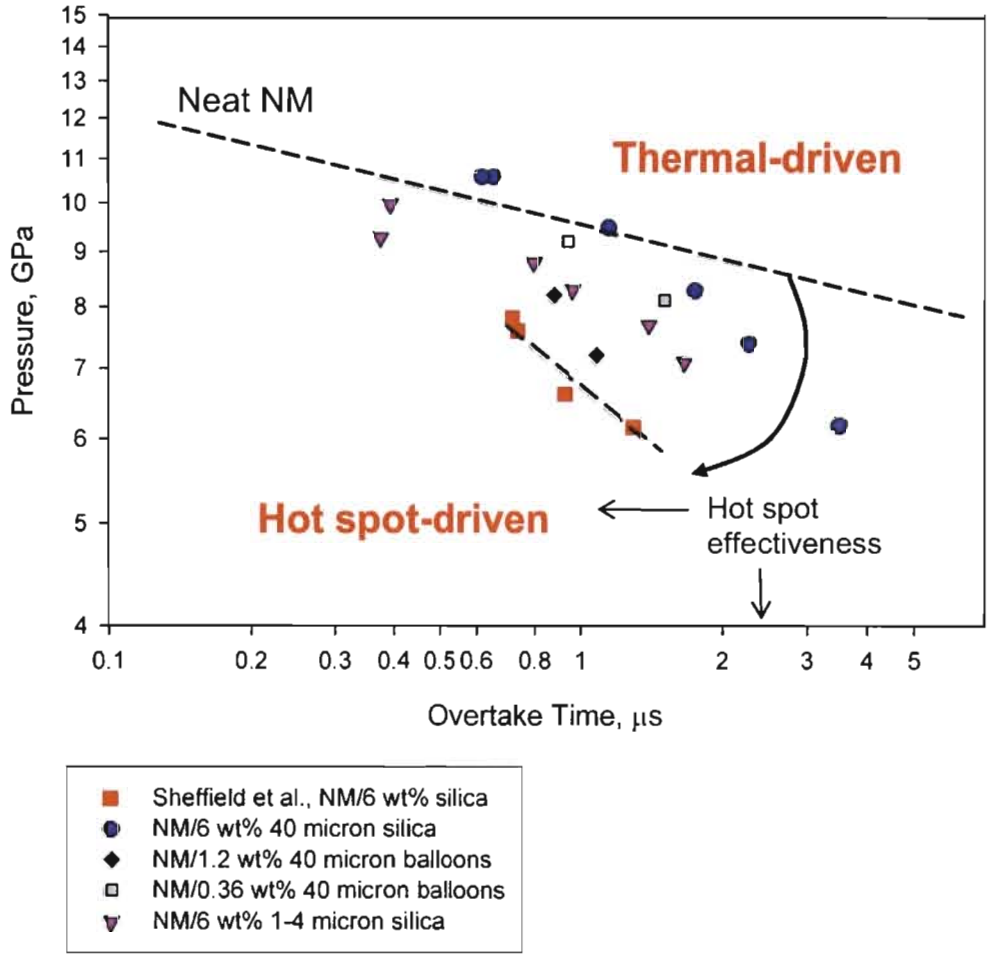

Conclusions

- There is a range of initiation behaviors from "homogeneous" to "heterogeneous" - *effectiveness of hot spots is the difference*

- We have studied two types of hot spots – impedance mismatches and void collapse – and their influence on shock initiation sensitivities and mechanisms

- A balance of initiation behaviors (thermal-driven vs. hot spot-driven) exists that is based on hot spot number density, size, and shock input strength (time).

- Microballoons or porosity is more sensitizing than impedance mismatches of same size/number density

- When the hot spots are not effective, the initiation behavior "returns" to that of neat NM (homogeneous, parallels Pop-plot).

From a shock physics perspective, reaction is indicated by the mechanical variables associated with the shock event.

$\rho_{products} > \rho_{reactants}$ $\rho_{products} = \rho_{reactants}$ $\rho_{products} < \rho_{reactants}$

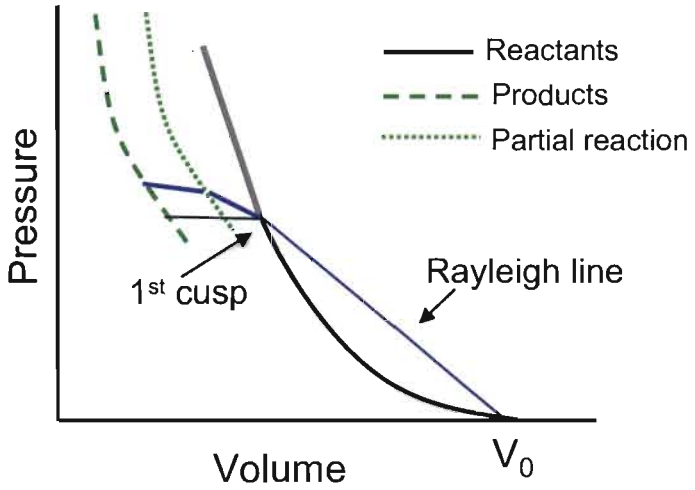

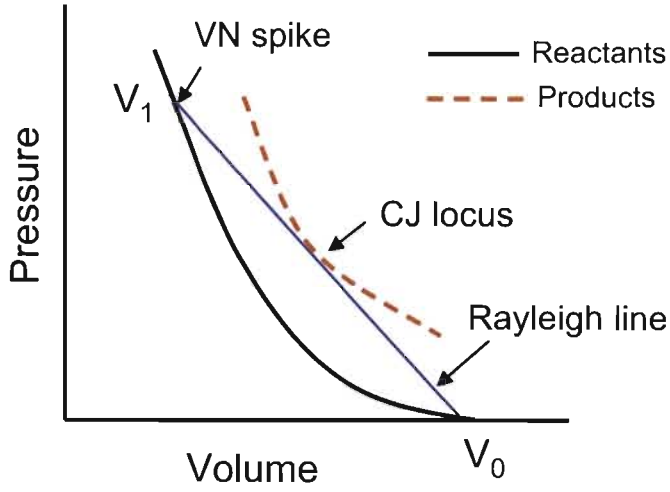

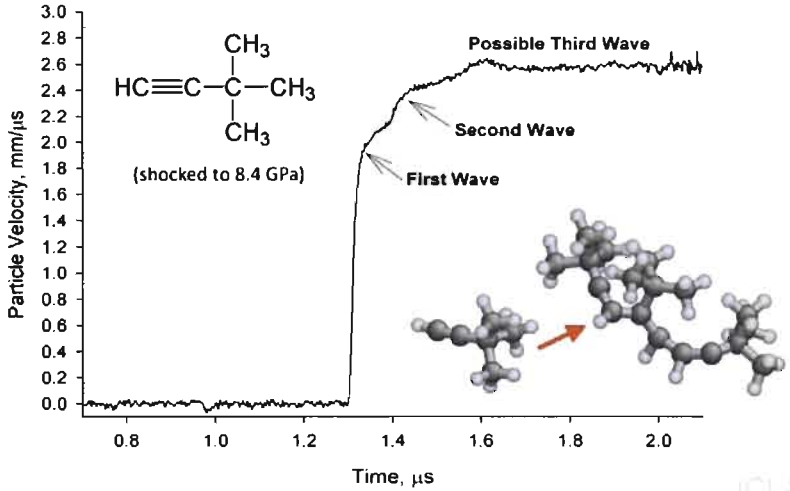

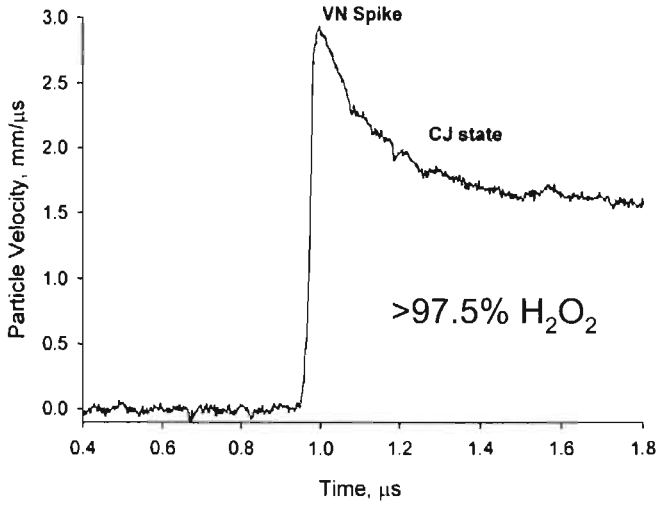

Shock wave profiles give the details of reactive flow – similar to solid-solid phase transitions.

- Organics with Hugoniot Cusps **(Products more dense than reactants)**
  - Liquid Organics (CS_2, benzene, toluene – data from R. Dick)
  - Polymers (Carter and Marsh) 20-25 GPa

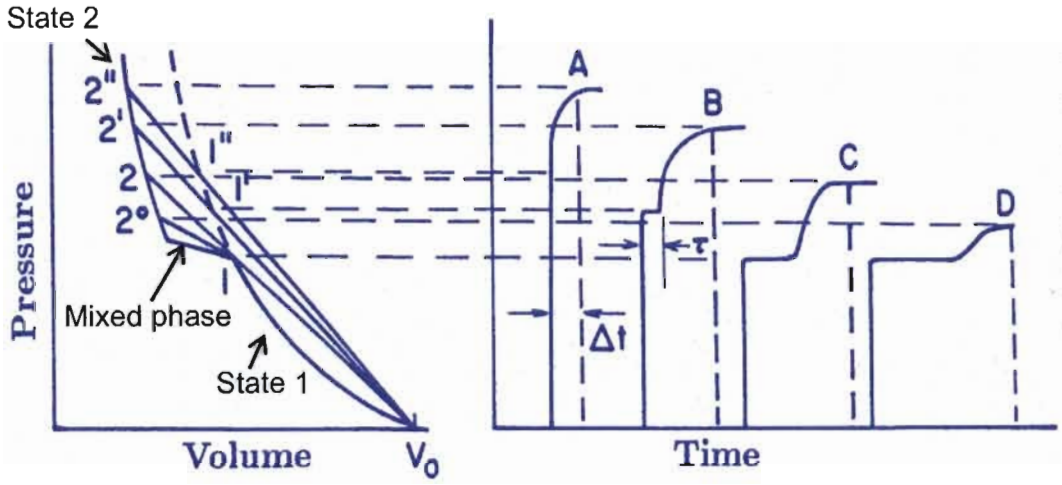

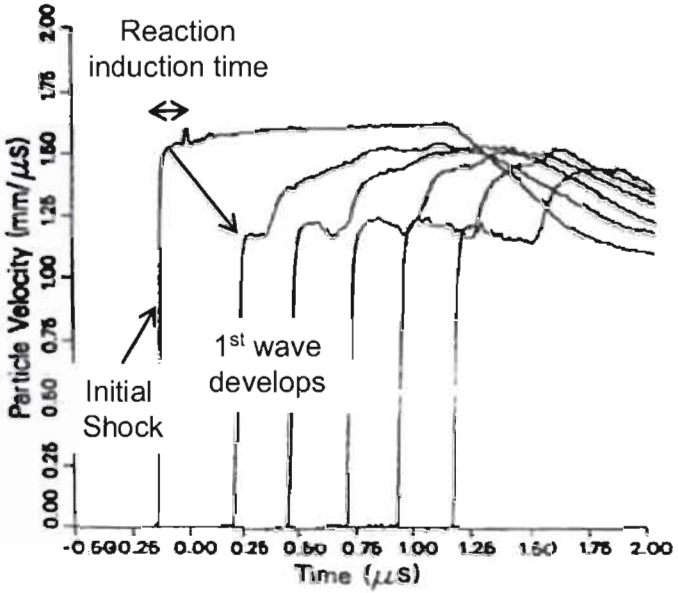

Example: phenylacetylene

- Shock velocity proportional to $(-\Delta P/\Delta V)$ – shock splits
- Increasing shock input - shocks directly to state 2
- Kinetic information from profile evolution
- Predicts steady notched wave – analogous to detonation

After Dremin et al. 1965 (applied to KCl and KBr)

We chose substituted acetylenes to probe differences in bond reactivity under shock compression.

Ethynyl trimethylsilane

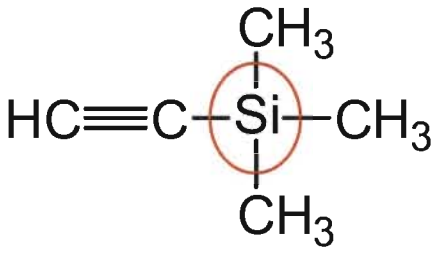

MW = 98.22 g/mol
b.p. = 52 °C
Density = 0.709 g/cm^3
Sound Speed^{22C} = 0.94 mm/μs

Tert-butylacetylene

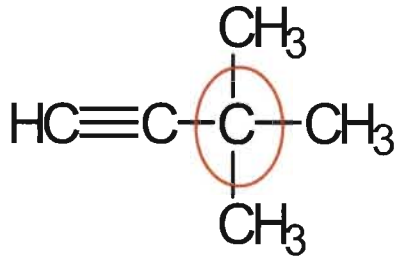

MW = 82.15 g/mol
b.p. = 37-38 °C
Density = 0.667 g/cm^3
Sound Speed^{22C} = 0.99 mm/μs

Phenylacetylene

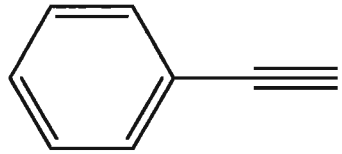

MW = 102.13 g/mol
b.p. = 143°C
Density = 0.928 g/cm^3
Sound Speed^{22C} = 1.39 mm/μs

S. A. Sheffield, D. M. Dattelbaum et al. AIP Conference Proceedings, 2005.

A pronounced multi-wave structure was observed in phenylacetylene

Shock-induced reaction observed in phenylacetylene

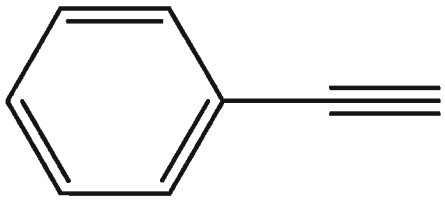

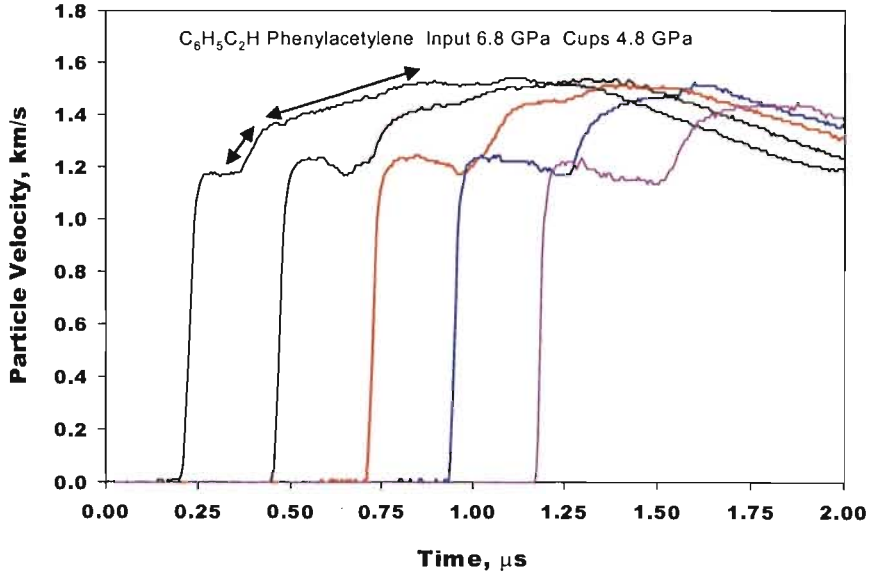

- From shot with shock input of 6.2 GPa
- Cusp observed at 4.8 GPa
- From interface – induction time = 0.13 μs
- Reactive wave - global rates

From Interface Particle Velocity
Induction Time -- 0.13 μs
Interface Decay Time -- 0.15 μs (6.7 μs^{-1})

From Multiple Embedded Gauges
1st Reaction -- 0.070 μs (14μs^{-1})
2nd Reaction -- 0.35 μs (2.8 μs^{-1})

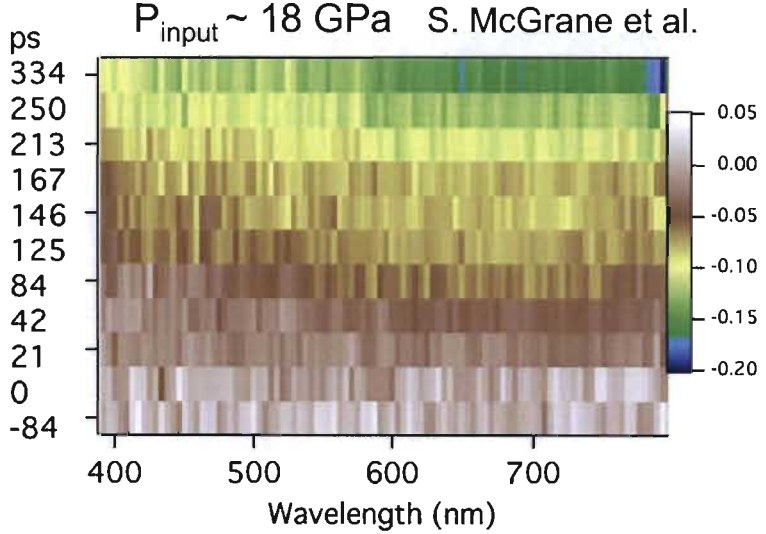

Sheffield, S. A.; Alcon, R. R. SCCM, 1990, p. 683.

Reaction was observed in the substituted acetylenes at higher pressures – greater than 6 GPa.

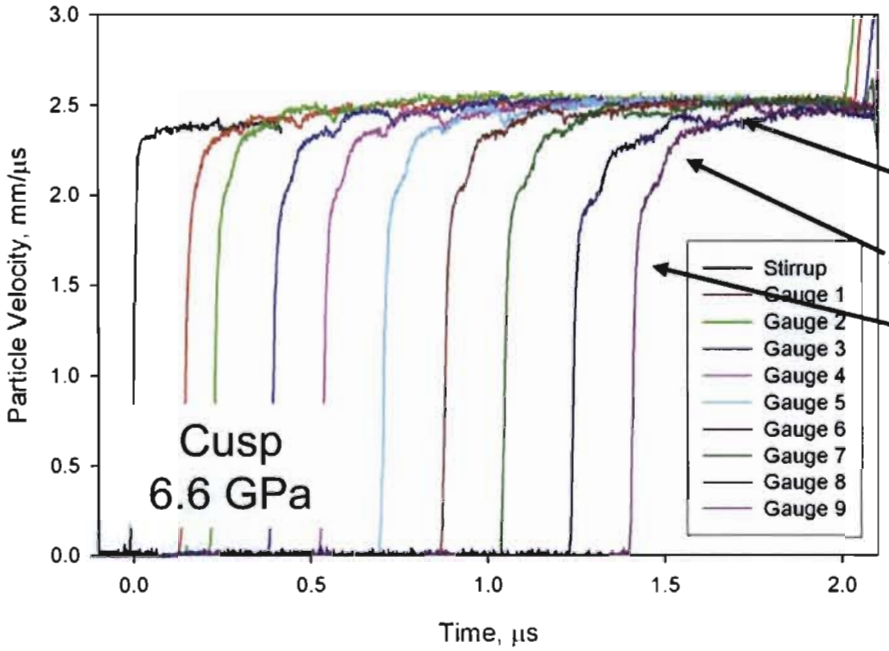

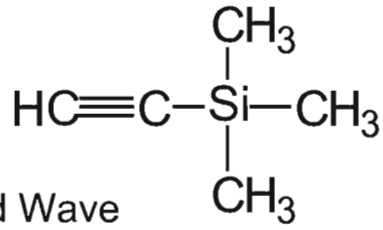

T ~ 700-800 K

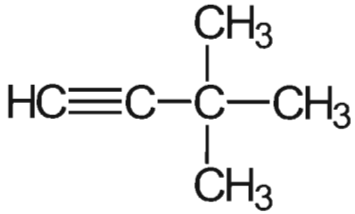

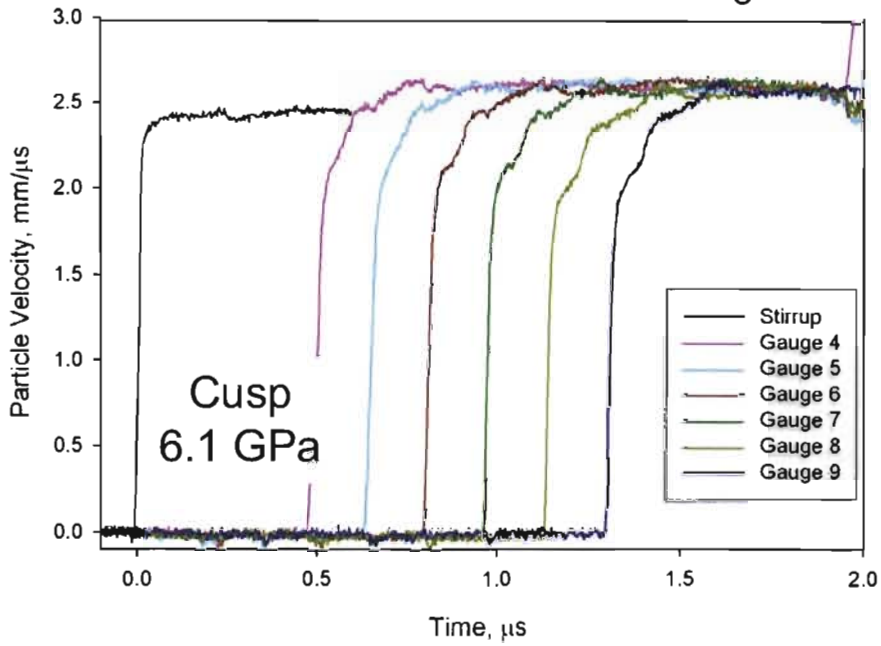

We observed 3-wave reactive structures indicative of 2-step reactions.

Two "fast" reactions – 14 μs^{-1} and 6 μs^{-1}
First step – reaction rate similar to phenylacetylene

We can compare the compressive energy to the cusp for all three acetylenes.

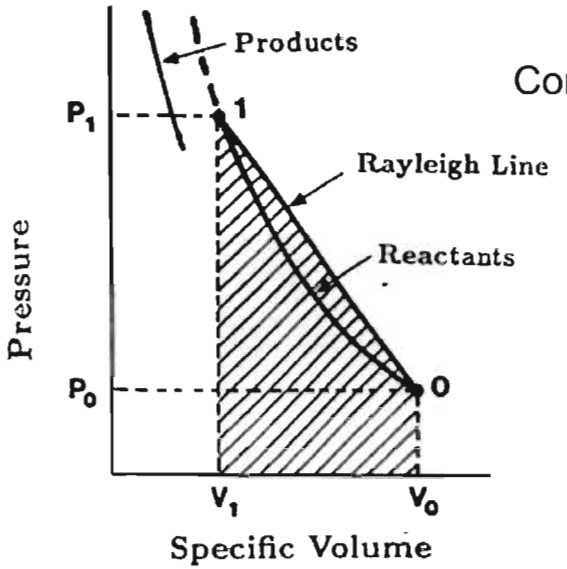

Compression Energy = $\frac{1}{2}(P_1 + P_0)(V_0 - V_1) = \frac{1}{2} P_1 \Delta V$

Internal energy rise behind shock

Determined by Hugoniot measurements to cusp pressure

ETMS @ Cusp
$\frac{1}{2}P\Delta V$ = 2.02 GPa cm^3/g

TBA @ Cusp
$\frac{1}{2}P\Delta V$ = 1.99 GPa cm^3/g

Energies are almost identical.

PA @ Cusp
$\frac{1}{2}P\Delta V$ = 0.72 GPa cm^3/g

Input energy is significantly less.

Electron donating/withdrawing capabilities –
TMS and tBu are similar electron donors, phenyl group is electron withdrawing

Embedded gauging provides detailed insights into the mechanical variables associated with shock-induced chemical reactions.

- Reaction under single shock conditions occurs at lower threshold pressures than under static conditions – temperature, lack of freezing, favored in conjugated structures

- Induction times and global rates point to "nanosecond" timescale chemistry (for full reaction) at moderate cusp pressures

- Evidence for reaction is derived from mechanical variables, need to quantify details from profiles

- Future directions must include comparing variety of shock and static conditions, coupling with spectroscopic techniques

Conclusions

- Embedded electromagnetic gauges have resulted in number of advances in shock and detonation physics – most notable is understanding details of shock initiation of explosives

- Unique and useful method for monitoring in-situ evolution of shock waves over ns-μs timescales

- Advantages – lack of calibration, robustness, flexibility, reasonable temporal resolution
- Disadvantages – expense, applicability to certain samples, expertise in data interpretation/error

Acknowledgments

- LANL Laboratory Directed Research and Development Program (projects # 20080015DR and #20110012DR) and project team members
- Other DOE/NNSA and DoD program sponsors
- Current and past Chamber 9 gas gun team members:

  David Stahl, Brian Bartram, Lee Gibson, Adam Pacheco, Rick Alcon, Richard Martinez, Joe Lloyd, Bob Medina

Extra slides

Lead circuit

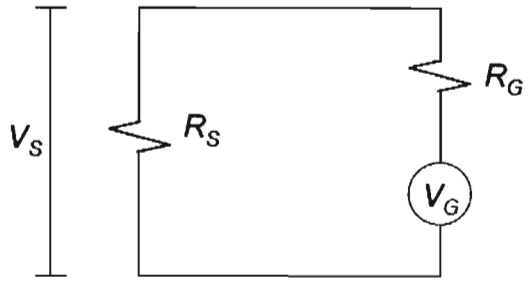

$$V_s = \frac{V_G R_s}{R_G + R_s}$$

V_s : Oscilloscope voltage (V)

V_G : Voltage generated by stirrup gauge (V)

R_s : Oscilloscope resistance (Ω)

R_G : Gauge and cable run resistance (Ω)

Influence of hot spots on initiation behaviors of energetic materials is dramatic.

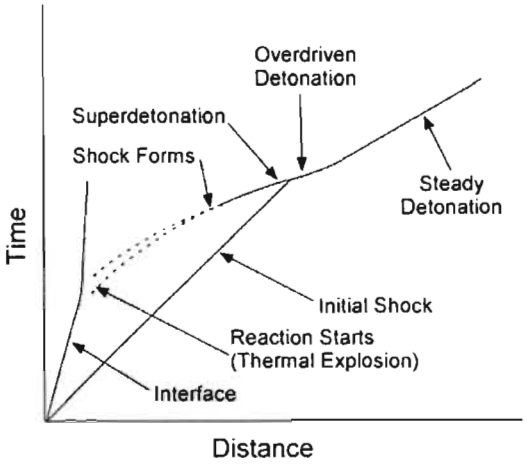

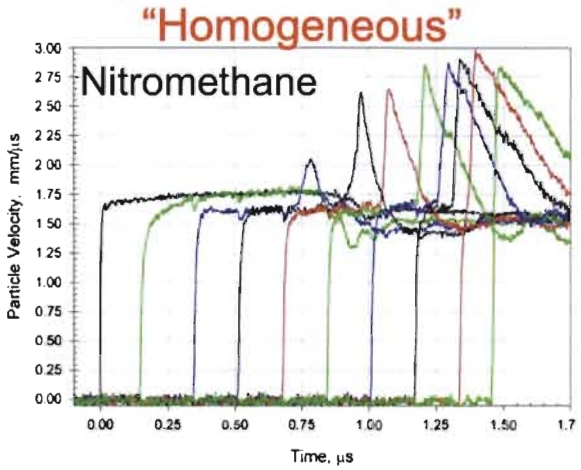

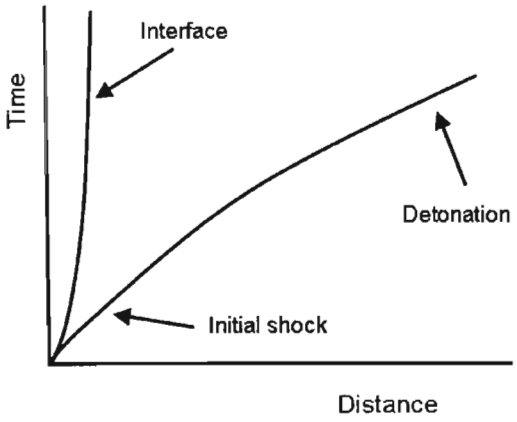

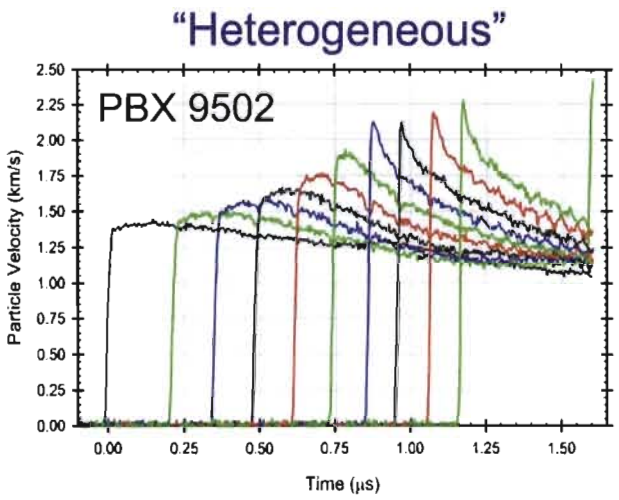

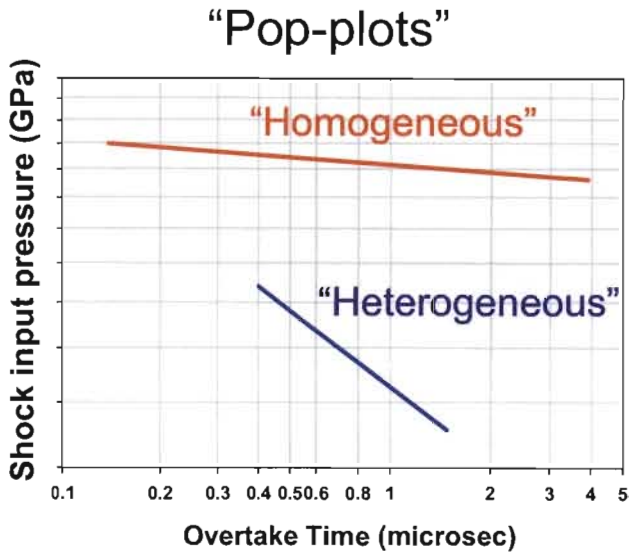

Campbell, Davis and Travis (1961)
Chaiken (1958, 1960)
Sheffield and Alcon (1989)

Ramsay, J. B.; Popolato, A. Fourth Symposium (Int.) on Detonation, Office of Naval Research Report # ACR-126, p 233 (1965).

Non-reactive reference state for liquids can be estimated using the "universal" liquid Hugoniot relationship.

"Universal" Liquid Hugoniot
Woolfolk, Cowperthwaite, Shaw at SRI
(Thermochimica Acta, 5(1973), 409-414)

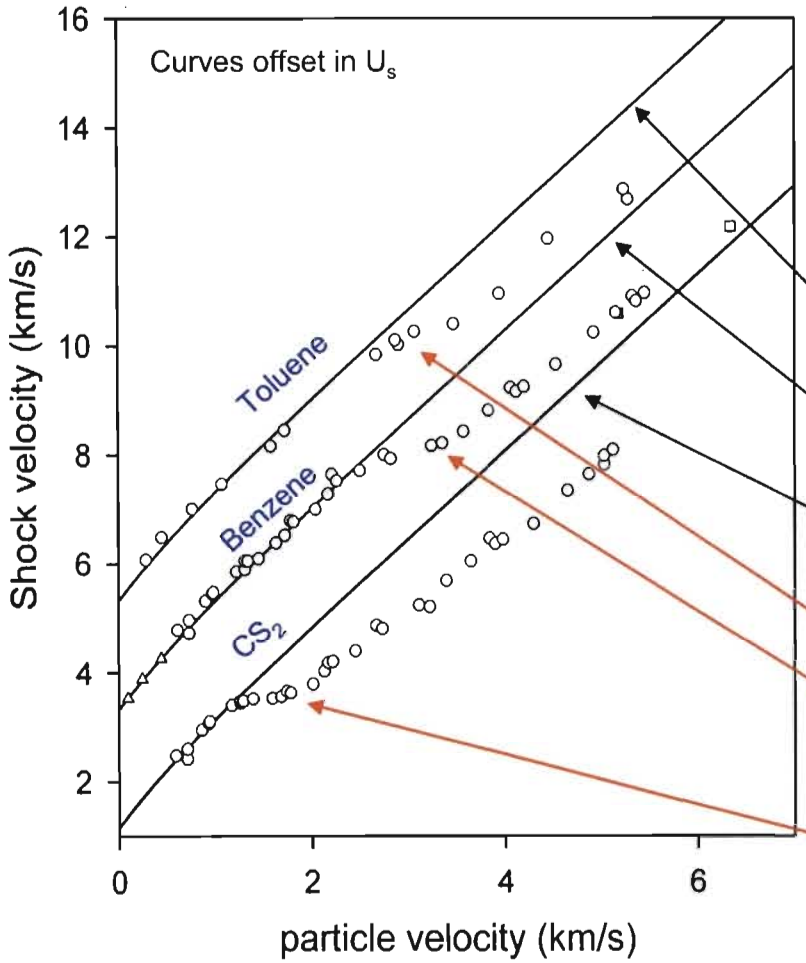

$$U_S = 1.37C_0 - 0.37C_0 e^{-(2u_p/C_0)} + 1.62u_p$$

where

U_S *is shock velocity,*

C_0 *is initial condition sound speed,*

u_p *is particle velocity.*

- Only requires measurement of bulk sound velocity at ambient conditions
- Many historical exp'ts measured U_s of 1st wave

"Universal" Liquid Hugoniot
Toluene – C_0 = 1.31 mm/μs
Benzene – C_0 = 1.31 mm/μs
Carbon Disulfide – C_0 = 1.16 mm/μs

Hugoniot Cusp
Toluene = 13 GPa
Benzene = 13 GPa
Carbon Disulfide = 5 GPa

R. D. Dick, "Shock Wave Compression of Benzene, CS_2, CCl_4 and Liquid Nitrogen, LA-3915. Additional benzene data by Walsh and Rice, and Cook and Rodgers not plotted.

Comparison of static and shock conditions – high pressure chemistry

Santoro, Ciabini, Bini, Schettino, J.
Raman Spectroscopy, 2003, p. 557-566.

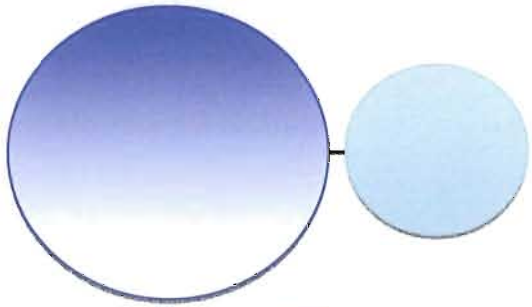

Benzene

- Reacts from crystalline phase > 23 GPa
- Formation of a-C:H (sp^3 bonds)
- excitation into S_1 lowers reaction pressure

Acetylene

- Reacts from Cmca phase at 4 GPa
- Polymerizes along diagonal of bc-plane
- Forms red trans-polyacetylene

Phenylacetylene

- Crystallizes at 1.1 GPa
- Begins to polymerize at 8.4 GPa
- Formation of orange polyphenylacetylene
- Phenyl ring remains intact

Acetylene moiety reacts first under static high pressure

Reaction pressure threshold is lowered by 3.6 GPa under shock compression.

In all cases, reaction is enhanced by excitation into singlet states.

We have just started to investigate polymerization reactions in TBA and ETMS.

Cryogenic Loading → TBA (orthorhombic) → Metastable to 10 GPa

Cryogenic Loading → ETMS ($P2_1$, monoclinic) → Opaque solid *polymerization 26.8 GPa*

Metastable low T phases

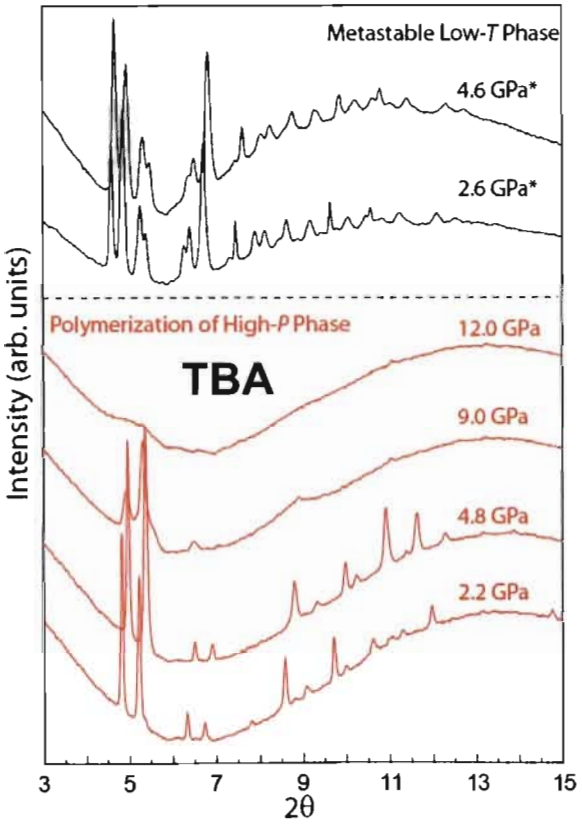

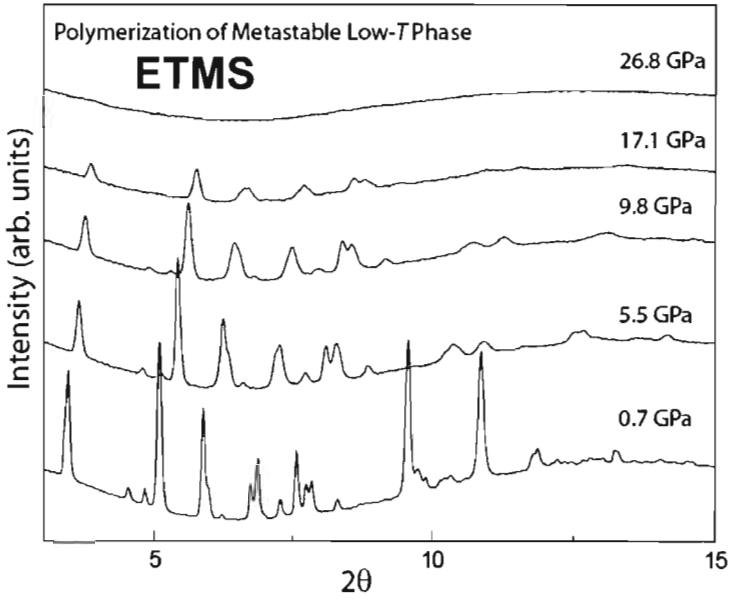

Fluid Loading → *Solidifies 1.5-2.6 GPa* → TBA (orthorhombic) → **High P phase** → Transparent glassy solid *polymerization 11 GPa*

Synchrotron XRD at APS

Each explosive has a different reaction zone length, and characteristics associated with the build-up to detonation.

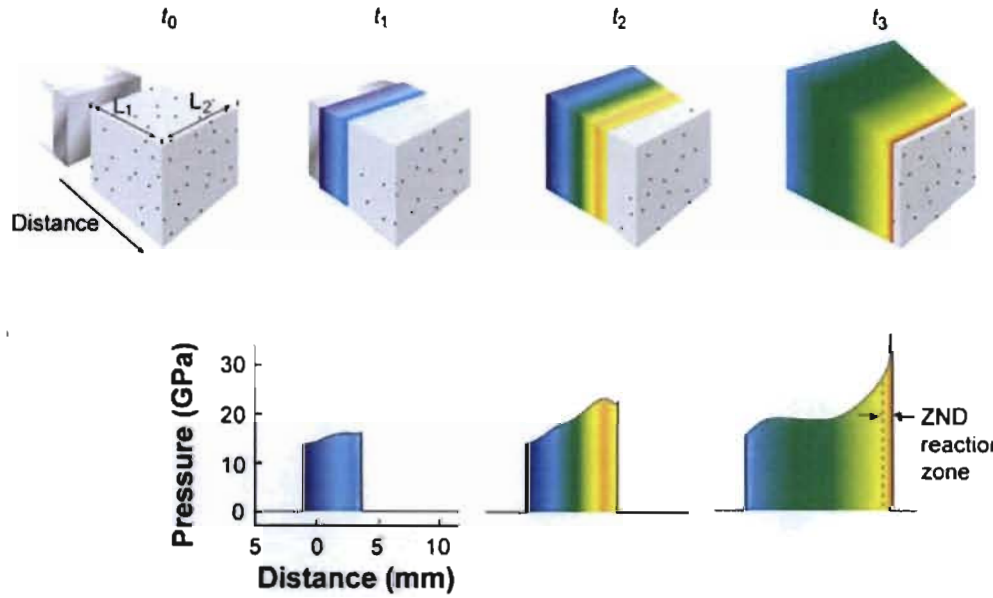

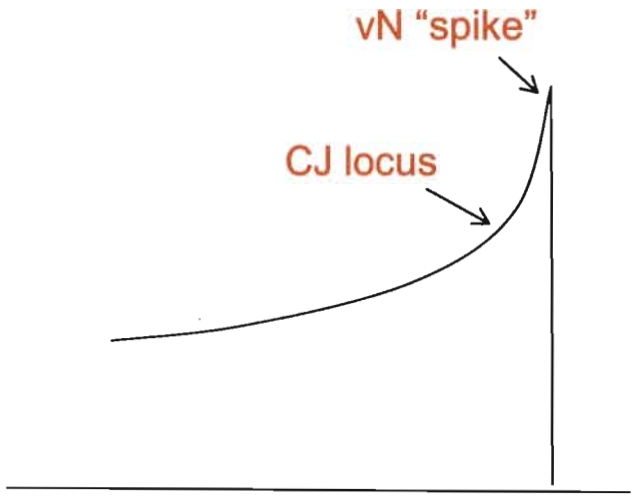

The chemical reaction zone "CRZ" is defined as the time/distance between vN spike and CJ locus.

The reaction zone dictates the failure characteristics of detonations and how they propagate in complex geometries (corner-turning).

*Bdzil & Stewart, Annu. Rev. Fluid Mech. **2007** 39:263-292*

UNCLASSIFIED

Influence of hot spots on initiation behaviors of energetic materials is dramatic.

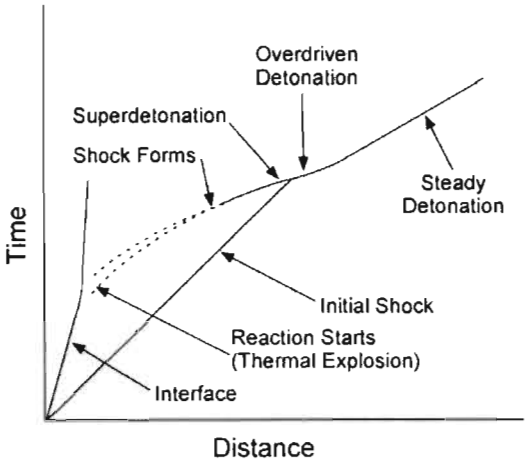

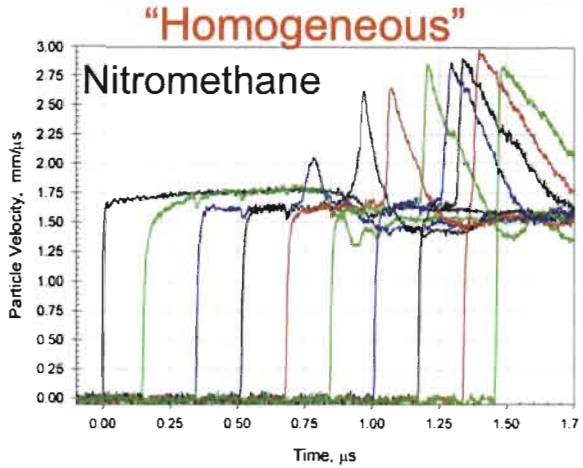

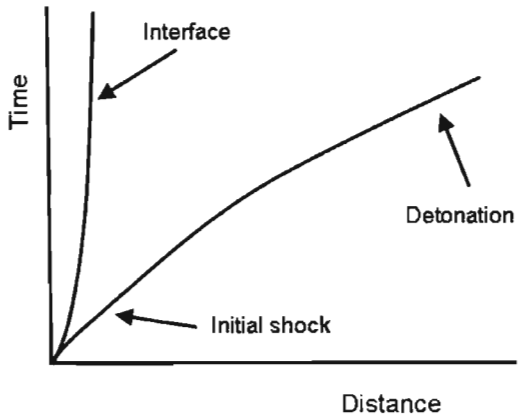

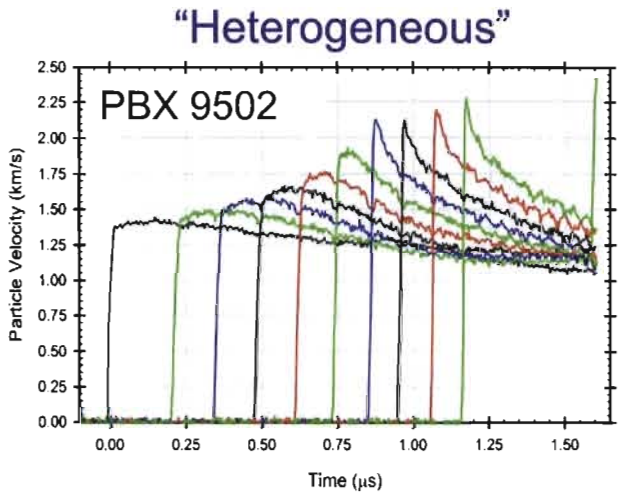

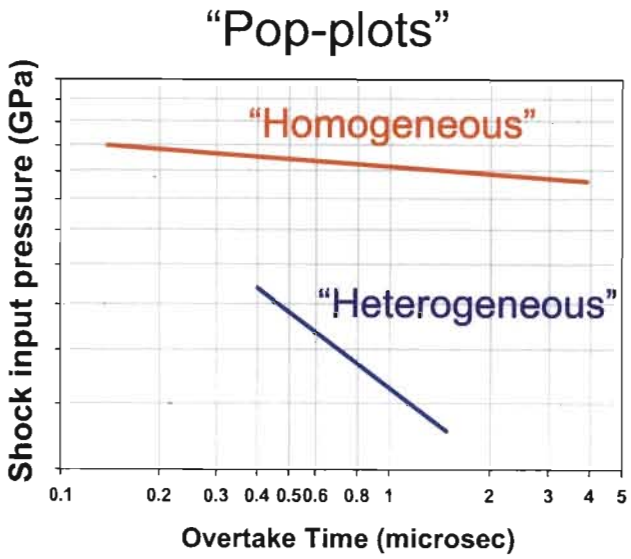

Campbell, Davis and Travis (1961)
Chaiken (1958, 1960)
Sheffield and Alcon (1989)

Ramsay, J. B.; Popolato, A. Fourth Symposium (Int.) on Detonation, Office of Naval Research Report # ACR-126, p 233 (1965).